

DEVELOPMENT OF GALLIUM-INDIUM ALLOYS AS NONMAGNETIC  
TEST MASSES FOR SPIN-DEPENDENT SHORT-RANGE FORCE  
EXPERIMENTS

Marjan Khosravi

Submitted to the faculty of Indiana University Graduate School in partial fulfillment of  
the requirements for the degree Master of Science in Department of Physics

Indiana University

December 2014

Accepted by the Graduate Faculty, Indiana University, in partial fulfillment of the  
requirements of the degree of Master of Science.

Master's Thesis Committee

---

W. Mike Snow, PhD.

---

Susan B. Klein, PhD.

---

Rick Van Kooten, PhD.

Dedicated to my Parents,  
who have supported me in every step of this journey.

## ACKNOWLEDGEMENTS

This thesis would not have been possible without the encouragement, support, and help of many people directly and indirectly involved in this research.

I would first like to acknowledge my research advisor Prof. Mike Snow for providing me the opportunity of research in his group, ensuring that the work is always on track, and also for serving on my thesis advisory committee. I could not have finished this research without his support and guidance.

I would also like to acknowledge my academic advisor, Dr. Susan Klein, not only for her professional guidance and support but also for her friendship and unselfish help whenever I needed through many difficult times during these two years, and also for serving on my thesis advisory committee. I am heartily thankful to Prof. Rick Van Kooten for his insightful advice and suggestions, and also for serving on my thesis advisory committee.

I could not have performed this research without the support of fellow graduate student Rakshya Khatiwada, whose assistance and support for this project is immeasurable. I am thankful for her help in many aspects of this project, not only understanding the theoretical background but also for her critical comments and concise suggestions. Many thanks also to Joel R. Kilzer for being my best friend.

Lastly, I own my deepest gratitude to my parents, Mostafa Khosravi and Mahin Haghghat Far. It has been your unconditional love and continuous support that has made all of this possible. Without you and your encouragement I would never achieve this far. This thesis is dedicated to you.

Marjan Khosravi

DEVELOPMENT OF GALLIUM-INDIUM ALLOYS AS NONMAGNETIC TEST  
MASSES FOR SPIN-DEPENDENT SHORT-RANGE FORCE EXPERIMENTS

Various studies have been done on exotic spin-dependent short-range forces in the mm to  $\mu\text{m}$  range. We are using an ensemble of optically polarized  $^3\text{He}$  gas and an unpolarized test mass to search for such forces. The presence or absence of a Nuclear Magnetic Resonance (NMR) frequency shift when an unpolarized mass is moved away and towards the  $^3\text{He}$  is our experimental signal [1]. It is very important to have no influence from the magnetism of the mass itself on the NMR frequency measurement. This research explicitly deals with preparation and characterization of unpolarized non-magnetic test masses using Gallium/Indium alloys that have very low magnetic susceptibility. We believe the current limit on the NMR frequency shift (ceramic  $2.6 \pm 1.7 \times 10^{-5}$  Hz, salt water  $(-0.8 \pm 2.6 \times 10^{-5})$  Hz) due to such spin-dependent forces from a previous experiment using Macor ceramic and 1.02%  $\text{MnCl}_2$  solution can be improved with the use of these lower magnetic susceptibility test masses.

## TABLE OF CONTENTS

|  | Pages |
|--|-------|
| TABLE OF FIGURES.....  | viii  |
| LIST OF ABBREVIATIONS.....   | x     |
| CHAPTER 1 – INTRODUCTION AND THEORY.....                                   | 1     |
| 1.1 – General Introduction.....  | 1     |
| 1.2 – Spin-Dependent Short-Range force Experiment (SDSRF).....             | 2     |
| 1.3 – Unpolarized Test Samples.....  | 5     |
| 1.4 – Medical Motivation.....  | 7     |
| CHAPTER 2 – OBJECTIVE OF THE STUDY.....                                    | 9     |
| CHAPTER 3 – METHODOLOGY.....   | 10    |
| 3.1 – Magnetic Susceptibility, $\chi$ .....                                | 10    |
| 3.2 – Why Gallium and Indium?.....   | 10    |
| 3.3 – Magnetic Susceptibility Balance (MSB).....                           | 11    |
| 3.4 – Additional Components to achieve the high level of sensitivity.....  | 13    |
| 3.5 – Gallium-Indium Alloy Synthesis.....                                  | 14    |
| 3.6 – Water as the Reference for Magnetic Susceptibility Measurements..... | 16    |
| CHAPTER 4 – RESULTS AND DISCUSSION.....                                    | 17    |
| 4.1 – Alloy Measurements for Synthesis.....                                | 17    |
| 4.2 – Water Susceptibility Measurements.....                               | 19    |
| 4.3 – Ga- In Alloys Measurements.....                                      | 22    |
| 4.4 – Discussion.....  | 38    |
| LIST OF REFERENCES.....  | 40    |

Curriculum Vitae (CV).....

## TABLE OF FIGURES

|   | Pages |
|---|-------|
| Figure 1- Schematic of SDRF experiment in phase I .....   | 4     |
| Figure 2- Schematic of SDRF experiment in phase II.....   | 5     |
| Figure 3- Constraints on the coupling strength $g_s g_p^n$ as a function of the force range $\lambda$ . ... | 6     |
| Figure 4- Johnson Matthey MSB device .....  | 12    |
| Figure 5- Additional components for higher sensitivity level achievements .....                             | 12    |
| Figure 6- MSB device positioned in the mu-metal shielding .....   | 13    |
| Figure 7- Two axis tilt sensor, Pitch and Roll .....  | 14    |
| Figure 8- A syringe used to dispense the alloy into NMR tubes .....   | 16    |
| Figure 9- Fluctuations of $\chi$ and T over 60 seconds for water measurements.....                          | 20    |
| Figure 10- Tilt measurement of Roll axis for water over 60 seconds.....                                     | 21    |
| Figure 11- Tilt measurement of Pitch axis for water over 60 seconds .....                                   | 21    |
| Figure 12- Magnetic susceptibility measurements for Ga-In 5% In over 60 (s) .....                           | 25    |
| Figure 13- Magnetic susceptibility measurements for Ga-In 10% In over 60 (s) .....                          | 26    |
| Figure 14- Magnetic susceptibility measurements for Ga-In 12% In over 60 (s) .....                          | 26    |
| Figure 15- Magnetic susceptibility measurements for Ga-In 13.4% In over 60 (s) .....                        | 27    |
| Figure 16- Magnetic susceptibility measurements for Ga-In 16.5% In over 60 (s) .....                        | 27    |
| Figure 17- Temperature measurements for Ga-In, 5% In alloy over 60 (s) .....                                | 28    |
| Figure 18- Temperature measurements for Ga-In, 10% In alloy over 60 (s) .....                               | 28    |
| Figure 19- Temperature measurements for Ga-In, 12% In alloy over 60 (s) .....                               | 29    |
| Figure 20- Temperature measurements for Ga-In, 13.4% In alloy over 60 (s) .....                             | 29    |
| Figure 21- Temperature measurements for Ga-In, 16.5% In alloy over 60 (s) .....                             | 30    |



|  |    |
|--|----|
| Figure 22- Tilt measurements of Roll axis for Ga-In 5% In over 60 (s) .....      | 31 |
| Figure 23- Tilt measurements of Pitch axis for Ga-In 5% In over 60 (s) .....     | 31 |
| Figure 24- Tilt measurements of Roll axis for Ga-In 10% In over 60 (s) .....     | 32 |
| Figure 25- Tilt measurements of Pitch axis for Ga-In 10% In over 60 (s) .....    | 32 |
| Figure 26- Tilt measurements of Roll axis for Ga-In 12% In over 60 (s) .....     | 32 |
| Figure 27- Tilt measurements of Pitch axis for Ga-In 12% In over 60 (s) .....    | 33 |
| Figure 28- Tilt measurements of Roll axis for Ga-In 13.4% In over 60 (s) .....   | 33 |
| Figure 29- Tilt measurements of Pitch axis for Ga-In 13.4% In over 60 (s) .....  | 33 |
| Figure 30- Tilt measurements of Roll axis for Ga-In 16.5% In over 60 (s) .....   | 34 |
| Figure 31- Tilt measurements of Pitch axis for Ga-In 16.5% In over 60 (s) .....  | 34 |
| Figure 32- Average magnetic susceptibility Vs. Indium Concentration.....         | 35 |
| Figure 33- Magnetic susceptibility Vs. In Concentration with Polynomial fit..... | 36 |
| Figure 34- Magnetic susceptibility Vs. In Concentration with Linear fit.....     | 37 |

## LIST OF ABBREVIATIONS

The following table describes the significance of various abbreviations and acronyms used throughout the thesis. The page on which each one is defined or first used is also given.

Table 1- List of Abbreviations

| Abbreviation            | Meaning   | Page |
|-------------------------|---|------|
| <b>ALP</b>              | Axion-Like Particles  | 2    |
| <b>Amg</b>              | Amagat, a practical unit of number density (1 atmosphere =0.923 amg)  | 3    |
| <b>cgs-emu</b>          | Centimeter-gram-second system-Electromagnetic unit<br>A unit of magnetic susceptibility (1 emu = 1 $cm^3$ )       | 9    |
| <b>cGSM/g</b>           | cgs electromagnetic system per mass unit, used for mass magnetic susceptibility (cgs and cGSM are the same units) | 10   |
| <b>Ga-In</b>            | Gallium-Indium Alloy  | 8    |
| <b>mG</b>               | Milli-gause equals $10^{-3}$ gause  | 12   |
| <b>mK</b>               | Milli-Kelvin equals $10^{-3}$ Kelvin (K)  | 11   |
| <b>MnCl<sub>2</sub></b> | Manganese (II) Chloride   | 4    |
| <b>Mrad</b>             | Milli-Radian  | 11   |
| <b>MSB</b>              | Magnetic Susceptibility Balance   | 6    |
| <b>NMR</b>              | Nuclear Magnetic Resonance  | ix   |
| <b>PTFE</b>             | Polytetrafluoroethylene used as Teflon coating  | 12   |
| <b>RF</b>               | Radio frequency   | 7    |
| <b>SDRF</b>             | Spin-Dependent Short-Range Force Experiment   | 2    |
| <b>Mm</b>               | Micro meter equals $10^{-6}$ meter (m)  | 3    |

Marjan Khosravi

DEVELOPMENT OF GALLIUM-INDIUM ALLOYS AS NONMAGNETIC TEST  
MASSES FOR SPIN-DEPENDENT SHORT-RANGE FORCE EXPERIMENTS

Various studies have been done on exotic spin-dependent short-range forces in the mm to  $\mu\text{m}$  range. We are using an ensemble of optically polarized  $^3\text{He}$  gas and an unpolarized test mass to search for such forces. The presence or absence of a Nuclear Magnetic Resonance (NMR) frequency shift when an unpolarized mass is moved away and towards the  $^3\text{He}$  is our experimental signal [1]. It is very important to have no influence from the magnetism of the mass itself on the NMR frequency measurement. This research explicitly deals with preparation and characterization of unpolarized non-magnetic test masses using Gallium/Indium alloys that have very low magnetic susceptibility. We believe the current limit on the NMR frequency shift (ceramic  $2.6 \pm 1.7 \times 10^{-5}$  Hz, salt water  $(-0.8 \pm 2.6 \times 10^{-5})$  Hz) due to such spin-dependent forces from a previous experiment using Macor ceramic and 1.02%  $\text{MnCl}_2$  solution can be improved with the use of these lower magnetic susceptibility test masses.

# CHAPTER 1 – INTRODUCTION AND THEORY

## 1.1 – General Introduction

- Symmetries Conservation and Violation

Scientists have studied symmetries to understand nature and the world around us, since early research in physics and more recently, symmetries have become the backbone of the theoretical formulation of physics. The validity of a symmetry principle relies on the non-observation of some type of process. A violation of symmetry becomes apparent when an observable constrained to be zero by the symmetry emerges to be observable. At this point the symmetry violation is discovered. We should consider that some unobserved quantities might be due to the limitations of our current ability to measure some symmetry violating signals. As the experimental techniques are improved, the domain of the observation increases and it is always possible that the violation of a new symmetry might be uncovered. There are three symmetry principles in nuclear science and subatomic physics:

- Space inversion  $P$ : The asymmetry of physics laws under space inversion  $r \rightarrow -r$ , also called right-left mirror transformation and denoted  $P$  for Parity.
- Time-reversal symmetry  $T$ : The laws of physics are identical when time is running backwards, i.e.,  $t \rightarrow -t$ .
- Particle-antiparticle Conjugation  $C$ .

The  $CPT$  theorem is based on Lorentz invariance in which  $T$  violation is equivalent to  $CP$  violation and can be called either  $T$  violation or  $CP$  violation.  $P$

violation was suggested by Lee and Yang in 1956 and  $T$  violation is as suggested in 1957 [2]. Recent studies on existence of short-range forces between polarized  ${}^3\text{He}$  nuclei and an unpolarized mass have searched for a possible new source for parity and time reversal symmetry violation [1].

### 1.2 – Spin-Dependent Short-Range Force Experiment (SDSRF)

The possibility of the existence of macroscopic forces with weak couplings and with force ranges from cm to  $\mu\text{m}$  has been proposed by several authors [3]. Moody and Wilczek [4] proposed a form of interaction due to the exchange of spin-0 bosons that couple to fermions through scalar and pseudoscalar vertices. The spin-dependent scalar coupling depends only on fermion density while the pseudoscalar coupling is completely spin-dependent [1]. The form of the resulting spin-dependent short range force (SDSRF) has a Yukawa-type interaction potential:

$$V(r) = \frac{g_s g_p \hbar^2}{8\pi m_p} (\hat{\sigma} \cdot \hat{r}) \left( \frac{1}{r\lambda} + \frac{1}{r^2} \right) \exp(-r/\lambda) \quad (1)$$

where  $\hat{r}$  is the unit vector from the unpolarized particle to the polarized particle,  $\hat{\sigma}$  is the spin of the polarized particle,  $m_p$  is the polarized particle mass,  $c$  is the product of couplings of the scalar vertex in the unpolarized matter and the pseudoscalar vertex of the polarized particle, and  $\lambda$  is the range of the force. The SDSRF can change the precession frequency of a polarized nucleon. The potential of the form  $\hat{\sigma} \cdot \hat{r}$  is similar to the potential of a magnetic dipole moment in an external magnetic field given by  $\vec{\mu} \cdot \vec{B}$  [5]. Such short-range forces can be induced by exchanging pseudoscalar bosons like axions or axion-like particles (ALP) between unpolarized nucleons and polarized nucleons. Based on current experimental observations, the axion mass is constrained to lie between 1  $\mu\text{eV}$  and 1

meV, corresponding to a force range between 2 cm and 20  $\mu\text{m}$ , the so called “axion window” [1]. It is therefore interesting to investigate this region with new experiments.

Several previous experiments have been devoted to searches for these interactions such as the torsion pendulum [6] and neutron bound states on a mirror in the earth’s gravitational field [7]. In the most recent work, performed in our lab, this force between nucleons was sought by considering the frequency shift of optically polarized  $^3\text{He}$  gas in the presence or absence of an unpolarized mass [3]. For this purpose, a 7 atm high pressure  $^3\text{He}$  cell that has an optical pumping chamber and a target chamber connected to a glass tube was designed to contain the polarized nuclei (Figure 1). The polarized  $^3\text{He}$  gas is maintained within a cylindrical cell constructed with two thin opposing glass windows; it is positioned at the center of a Helmholtz coil pair to retain the polarization. The thickness of the glass window is about 250  $\mu\text{m}$ , thin enough that we can search for forces with ranges in the sub-millimeter scale using test masses introduced from the outside.

The unpolarized mass was placed at the end of the cylindrical cell containing the polarized  $^3\text{He}$  gas. The mass was repeatedly brought into contact with (mass-in) and moved away from the cell (mass-out). No mass was placed at the other end of the cylindrical cell. Two identical pick up coils were placed just below each window. By comparing the precession frequency of the two ends of the cylinder and the difference between mass-in and mass-out, the effect of the short range force can be isolated.

As illustrated in Figure 1, pickup coil A measured the frequency of the polarized  $^3\text{He}$  nuclei affected by the mass while pickup coil B was effectively used as a magnetometer to monitor the magnetic holding field. The first measurement using this

method without any magnetic shielding resulted in a sensitivity of  $5 \times 10^{-3}$  Hz for the frequency shift over the force ranges from  $10^{-4}$  m to  $10^{-2}$  m, which corresponds to a mass range of  $2 \times 10^{-3}$  eV to  $2 \times 10^{-5}$  eV for the pseudoscalar bosons.

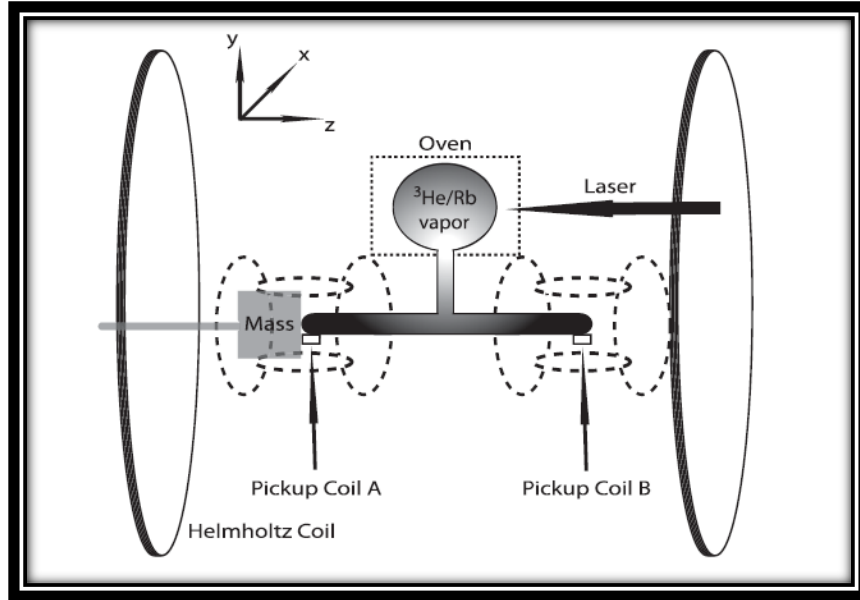


Figure 1- Schematic of SDRF experiment in phase I

In the second phase (phase II) of the experiment, shown in Figure 2, the two pickup coils were positioned closer to each other to enhance their correlation. With this new set up an upper bound with a factor 10-30 improvement was achieved on the sensitivity to the product of  $g_s g_p^n$  of the scalar couplings to the fermions in the unpolarized mass.

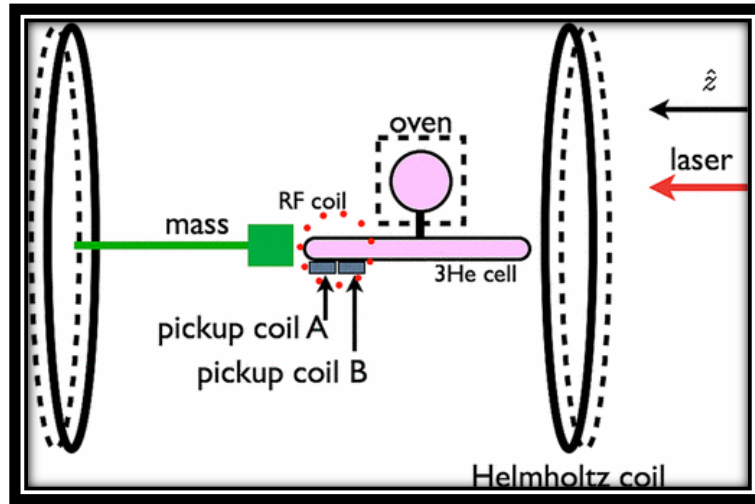


Figure 2- Schematic of SDRF experiment in phase II

### 1.3 – Unpolarized Test Samples

In the latest studies different unpolarized test masses have been used: a Macor ceramic mass block with dimensions of  $34 \times 52 \times 38 \text{ mm}^3$  [3] and a liquid mixture of 1.02%  $\text{MnCl}_2$  in pure water. For the samples, the NMR frequency shift is taken in two states; when the unpolarized mass was moved near the polarized  $^3\text{He}$  and when the unpolarized mass was moved away from the polarized  $^3\text{He}$ . Using the frequency shift difference, the constraint on the coupling strength and the force range can be seen in Figure 3. The darkened area has been ruled out by previous measurements. In this Figure, the constraints of  $g_s g_p^n$  with different values of  $\lambda$  are established and  $\log |g_s g_p^n|$  is plotted versus range of the force ( $\lambda$ ). The dotted curve is from reference [5] and the dash-dotted curve is from reference [8]. The solid black curve is the average constraint of the salt sample from reference [1]. The red curve is from reference [9] and the dashed curve that intersects the x-axis ( $\lambda$ ) is from reference [10]. The dashed solid curve is the constraint of the ceramic sample from reference [1].



The Macor ceramic mass block and liquid mixture of 1.02%  $\text{MnCl}_2$  were chosen for their low magnetic susceptibility and magnetic impurities, different nucleon densities, and minimal influence on the magnetic resonance (NMR) measurements procedure.

Despite the use of low magnetic susceptibility materials, the largest systematic error in the experiment will eventually come from the magnetism of the test masses: even normally “non-magnetic” test masses possess a magnetic susceptibility. Macor’s magnetic susceptibility is known to be small enough that it does not cause a systematic error in the previous experiments. However, real material can in principle contain paramagnetic or even ferromagnetic impurities.

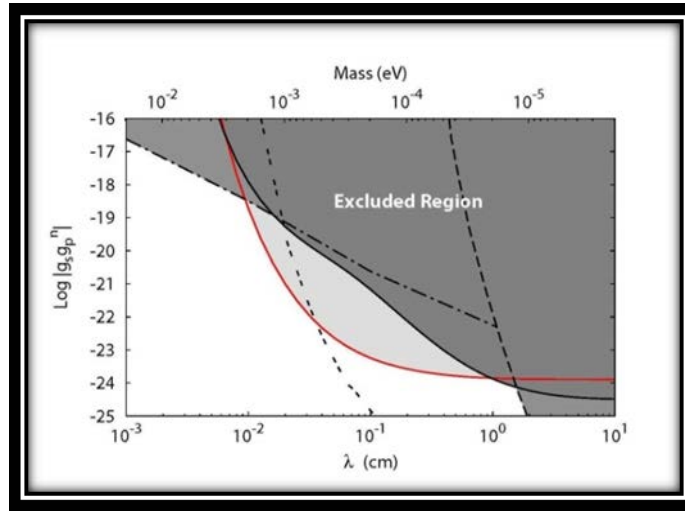


Figure 3- Constraints on the coupling strength  $g_s g_p^n$  as a function of the force range  $\lambda$ .

Therefore, one of the obvious paths for improvement of these measurements includes the use of unpolarized mass samples with lower magnetic susceptibilities. Liquid gallium has one of the smallest magnetic susceptibilities per unit mass of any pure elemental substance [11]. However, not all experimental apparatus can be operated at the temperature (slightly above room temperature) where the gallium is liquid. Thus, we

decided to study the magnetic properties of liquid Gallium-Indium alloys. With the addition of indium, the alloy becomes liquid at room temperature which is very convenient for experiments. To study the physical characteristics of Gallium-Indium alloys, a Johnson Matthey Magnetic Susceptibility Balance was used (MSB) [12]. The MSB is a mechanical torsion balance that determines the magnetic susceptibility of the solids and liquids. In 1974, Prof. D.F. Evans of Imperial College, London, developed a new type of MSB for semi-microscale samples [12]. Johnson Matthey's MSB functions are based on Professor Evans's design. MSB is used to measure a wide range of paramagnetic and diamagnetic materials. There are two models of MSB offered by the Johnson Matthey Company: Mark I which is mostly used in teaching applications and the MSB-Auto that we have used for this research.

#### 1.4 — Medical Motivation

NMR is the foundation for Nuclear Magnetic Resonance and the study of the magnetic properties of the nucleus of the atom. The same principles that are used herein to measure the magnetic properties of liquid Gallium-Indium alloys are used in imaging devices to visualize anatomy. Since the 1940s, NMR signal detection and analysis has been studied in chemistry and biochemistry as an analytical tool to provide spectroscopic data. In 1970s, it was realized that the NMR signal could be localized using magnetic field gradients to generate images. These images display magnetic properties of protons that can reveal useful clinical information. The increase of clinical imaging applications in 1980s resulted in elimination of the “nuclear” term and magnetic resonance imaging (MRI) was used in the medical community [13].

In NMR a static and homogenous magnetic field is imposed on the sample to align the axis of precession in an arbitrary direction. A second field which is perpendicular to the precession axis is then applied with an oscillating magnitude at the Larmor frequency. The fields are chosen to be perpendicular to maximize the NMR signal. The resonant nature of the second field exerts a torque that tips the angular momentum of the atom into a plane perpendicular to its original axis. Due to the higher energy of the new direction than that of the previous state, the nuclear moment of the atom decays to its original state [14]. The decaying atom releases the extra energy and emits photons. The emitted radiofrequency (RF) can be detected by a pickup coil that encodes specific spatial information. A Fourier transform is then used to deconvolve the information and construct the image in MRI.

## CHAPTER 2 – OBJECTIVE OF THE STUDY

The objective of this project is to develop unpolarized test masses whose magnetic susceptibility is as close as possible to zero in order to minimize the influence on the Nuclear Magnetic Resonance (NMR) measurement procedure used in the spin-dependent fifth force searches. The following tasks are prerequisites to the objective that will be addressed in this thesis:

- Development of liquid Gallium-Indium alloys, with 5, 10, 12, 13.4, 16.5 atomic percent Indium as non-magnetic test masses.
- Enhance the NMR measurement sensitivity of the Magnetic Susceptibility balance.
- Use the non-magnetic test masses for further searches on spin-dependent short-range forces.

## CHAPTER 3 – METHODOLOGY

### 3.1 – Magnetic Susceptibility, $\chi$

The magnetization  $\mathbf{M}$  induced at any point in a body is proportional to the strength of the applied magnetic field  $\mathbf{H}$  [15].

$$\mathbf{M} = \chi_v \mathbf{H} \quad (2)$$

where  $\chi_v$  is called the *volume magnetic susceptibility* [14]. Magnetic susceptibility depends on the nature of the material, the electronic structure of the atoms, and on the concentration and energy of conduction electrons [14, 16]. The volume magnetic susceptibility can be negative or positive. If the induced magnetic moment is parallel to the magnetic field, the substance is *paramagnetic* with positive susceptibility. The substance is said to be *diamagnetic* if the  $\chi_v$  is negative and the magnetic moment is anti-parallel to the applied magnetic field [14].

Volume magnetic susceptibility can be expressed in two different systems of units: either as SI or cgs-emu units.

### 3.2 – Why Gallium and Indium?

In this research study, we explicitly deal with the preparation and characterization unpolarized non-magnetic test masses using Gallium (Ga) and Indium (In) alloys with various weight percent Indium. The Ga-In, 16.5% In was chosen specifically to be studied due to the availability of previous information and results in the scientific literature [11]. The batches with other Indium percentage values were chosen for two reasons: 1- Lower percentages of In, i.e. greater amount of Ga, result in lower magnetic

susceptibility alloys, 2- The values of 5, 10, 12, 13.4 In percent belong to a region that has not been studied. Gallium is specifically chosen due to its low magnetic susceptibility. With addition of indium the mixture becomes liquid at room temperature and forms a homogeneous alloy.

Gallium belongs to group III of the periodic table. It has a low melting point of 29.78 °C with low vapor pressure [17]. Gallium has low diamagnetism, 0.248E-06 cGSM/g mass magnetic susceptibility in the solid phase, and very low paramagnetism,  $0.002 \times 10^{-6}$  cGSM/g mass magnetic susceptibility in the liquid phase [16].

Indium is a nontoxic element that belongs to group III of the periodic table with chemical characteristics similar to Gallium. It is a rare, soft and silvery-white metal with low melting point of 156.61 °C [17]. Solid Indium is diamagnetic with magnetic susceptibility of  $-0.112 \times 10^{-6}$  cGSM/g [16].

### 3.3 – Magnetic Susceptibility balance (MSB)

We performed accurate measurements of  $\chi_v$  using the MSB-Auto (Johnson Matthey) which is a portable device with high levels of sensitivity within the range of  $0.001 \times 10^{-7}$  to  $1.99 \times 10^{-4}$  cgs volume susceptibility units. The MSB device uses a stationary sample and two pairs of moving magnets on a torsion balance. The stationary sample, housed inside a NMR tube, is positioned between the two poles of one pair of the magnets. The torque induced by the magnetic susceptibility of the sample in the field gradient acts upon a suspended magnet. It is detected and is converted to a voltage signal using the feedback from a current in a coil immersed on the other side of the balance [12].



Figure 4- Johnson Matthey MSB device



Figure 5- Additional components for higher sensitivity level achievements

### 3.4 – Additional Components to achieve a high level of sensitivity

To achieve a higher level of sensitivity with the MSB-Auto (Johnson Matthey), it must be properly isolated from the environment. The device rests on a marble table for the greatest possible stability. Two concentric mu-metal cylinders were constructed as magnetic shielding. The space between the two shields is filled with polyethylene beads

for thermal insulation. Two temperature sensors with 1 mK resolution are used to record the temperature fluctuations both outside and inside the shielding. A two axis tilt sensor (Aosi Tilt EZ) shown in Figure 7 with 0.001 milliradian (mrad) sensitivity is used to verify that the torsion balance does not tilt during the measurement. The tilt sensor has a Roll (*R*) axis that monitors any rotation or tilt in *y*-axis, and the Pitch (*P*) axis that monitors any rotation or tilt in *x*-axis. A single axis fluxgate magnetometer (Bartington) with 1 mG sensitivity is used to measure the background magnetic field inside the shielding. The final sensitivity achieved for magnetic susceptibility measurements is  $0.001 \times 10^{-6}$  cgs.



Figure 6- MSB device positioned in the mu-metal shielding



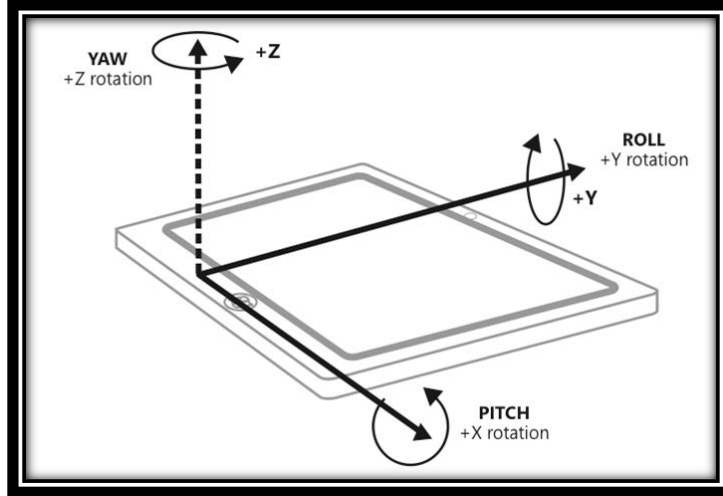


Figure 7- Two axis tilt sensor, Pitch and Roll

### 3.5 – Gallium-Indium Alloy Synthesis

The Gallium-Indium alloy was synthesized by heating a solution of 99.99% pure Ga (American Elements) and 99.99% pure In (American Elements). In the first step, the In atomic percent and Ga atomic percent values were converted to In weight % and Ga weight % values as summarized in Table 2. The desired amount of Ga and In was then calculated for each batch of samples considering the two constraints in Equations (3) and (4).

Table 2- Conversion of atomic % to wt. % for Ga and In

| In atomic % | Ga atomic % | In wt. % | Ga wt. % |
|-------------|-------------|----------|----------|
| 5           | 95          | 7.9761   | 92.0240  |
| 10          | 90          | 15.4676  | 84.5324  |
| 12          | 88          | 18.3383  | 81.6617  |
| 13.4        | 86.611      | 21.4175  | 78.5825  |
| 16.5        | 83.5        | 24.5520  | 75.4480  |

$$\frac{In \text{ wt.}\%}{7.31 \text{ (g / cm}^3\text{)}}\alpha + \frac{Ga \text{ wt.}\%}{5.904 \text{ (g / cm}^3\text{)}}\beta = 2 \text{ (ml)} \quad (3)$$

where  $\alpha$  is the amount of Indium in grams and  $\beta$  is the amount of Gallium in grams

$$\frac{\alpha}{\alpha + \beta} \times 100 = In \text{ wt.}\% \quad (4)$$

In the next step, the apparatus and equipment were cleaned with soap and distilled water and wiped down with disposable alcohol pads (VMR International, L.L.C) to remove all residues. The PTFE Teflon coated Pyrex Syringe inner tube (Western analytical Products Inc. [USA]), Teflon tubing (Western analytical Products Inc. [USA]), and glassware was washed with 10% hydrochloric acid (Fisher Scientific) and rinsed 4 to 5 times with distilled water. Finally, the inside and outside of all the equipment was washed and wiped with Acetone (EMD Chemicals) and air dried.

The sealed Gallium container was placed in a small ceramic container and partially submerged in hot water. Care was taken to assure that water did not seep inside the bottle. The melted Gallium was poured into the weighing pan (Lab Depot Inc.), weighed using a Balance weight with 0.0001 precision (Sartorius-Model CP224S) and poured into a 50 ml Borosilicate glass beaker (VMR International) to mix with the Indium at different atomic percentages. The pan was weighted again to measure the lost gallium. Each Indium-Gallium mixture was heated for about 17 minutes at 164°C on a digital laboratory hot plate with magnetic stirrer (VMR International) while stirring with a Teflon-coated magnetic disc stir bar (Big Science Inc.) at 800 rpm. The mixture was continuously stirred with a Teflon rod (Big Science Inc.) as well. To avoid Indium oxidation the temperature was kept lower than 200°C and the heating time was less than 30 minutes [18].

The mixture was left inside the oven (turned off) to cool uncovered to avoid water condensation on top of the molten alloy. A syringe with non-magnetic or non-metallic

components was used to dispense the room temperature alloy into NMR tubes (Johnson Matthey) and cleaned glass bottles for storage.

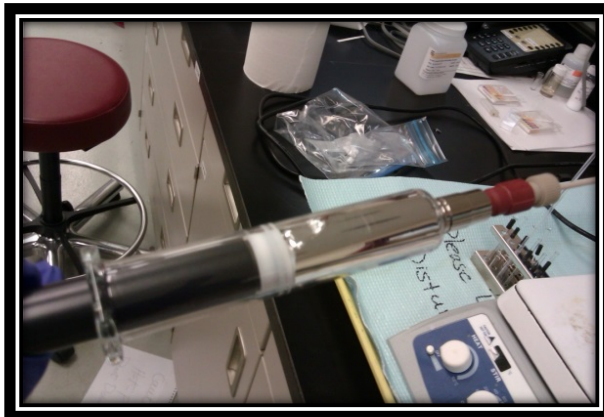


Figure 8- A syringe used to dispense the alloy into NMR tubes

### 3.6 – Water as the Reference for Magnetic Susceptibility Measurements

Water has a low diamagnetic susceptibility of  $-0.712 \times 10^{-6}$  [19], and was chosen as a reference for the susceptibility measurement. The magnetic susceptibility balance was calibrated with distilled water (EMD Chemicals) to check the stability and sensitivity of the balance and other sensors. The NMR tube filled with distilled water was then used for reference measurement for 60 seconds to check the MSB device accuracy. The already-cleaned NMR tubes were then filled with the Ga-In alloys with different percentages of Indium and were measured four times using the MSB.

## CHAPTER 4 – RESULTS AND DISCUSSION

### 4.1 – Alloy Measurements for Synthesis

The Ga-In alloys were synthesized with a slightly different mixture than planned as some Ga was lost during transfer to the beaker due to its stickiness. The tables 3-7 below summarize the calculated and measured values of In and Ga used for the synthesis of Ga-In alloy with 5, 10, 12, 13.4, 16.5 In wt. % respectively. As we see in Tables 3-7, the amount of Ga and In used in practice was slightly different than calculated.

Table 3- Calculated and Measured data for Ga- In. 5% In

| Material for Ga-In, 5% In | Weight (g)           |
|---------------------------|----------------------|
| Calculated Indium         | 1.10544              |
| Calculated Gallium        | 12.75406             |
| Measured Weighing Pan     | $0.8137 \pm 0.0002$  |
| Measured Pan plus In      | $1.9183 \pm 0.0002$  |
| Measured Actual Indium    | $1.1046 \pm 0.0031$  |
| Expected Beaker plus Ga   | 43.04716             |
| Measured Beaker plus Ga   | $43.0886 \pm 0.0002$ |
| Measured Actual Gallium   | $12.7955 \pm 0.0044$ |

Table 4- Calculated and measured data for Ga- In, 10% In

| Material for Ga-In, 10% In | Weight (g)           |
|----------------------------|----------------------|
| Calculated Indium          | 2.48865              |
| Calculated Gallium         | 13.6008              |
| Measured Weighing Pan      | $0.8357 \pm 0.0002$  |
| Measured Pan plus In       | $3.3229 \pm 0.0002$  |
| Measured Actual Indium     | $2.4872 \pm 0.0006$  |
| Expected Beaker plus Ga    | 43.8956              |
| Measured Beaker plus Ga    | $43.8979 \pm 0.0002$ |
| Measured Actual Gallium    | $13.6031 \pm 0.0002$ |

Table 5- Calculated and measured data for Ga- In, 12% In

| Material for Ga-In, 12% In | Weight (g)       |
|----------------------------|------------------|
| Calculated Indium          | 3.12004          |
| Calculated Gallium         | 13.8938          |
| Measured Weighing Pan      | 0.8204 ± 0.0001  |
| Measured Pan plus In       | 3.9414 ± 0.0002  |
| Measured Actual Indium     | 3.1210 ± 0.0002  |
| Expected Beaker plus Ga    | 44.5411          |
| Measured Beaker plus Ga    | 44.5432 ± 0.0002 |
| Measured Actual Gallium    | 13.8959 ± 0.0002 |

Table 6- Calculated and measured data for Ga- In, 13.4% In

| Material for Ga-In, 13.4% In | Weight (g)       |
|------------------------------|------------------|
| Calculated Indium            | 3.86357          |
| Calculated Gallium           | 14.1758          |
| Measured Weighing Pan        | 0.8304 ± 0.0002  |
| Measured Pan plus In         | 4.6939 ± 0.0002  |
| Measured Actual Indium       | 3.8651 ± 0.0457  |
| Expected Beaker plus Ga      | 44.4714          |
| Measured Beaker plus Ga      | 45.3358 ± 0.0002 |
| Measured Actual Gallium      | 15.0402 ± 0.0734 |

Table 7 -Calculated and measured data for Ga- In, 16.5% In

| Material for Ga-In, 16.5% In | Weight (g)        |
|------------------------------|-------------------|
| Calculated Indium            | 4.69166           |
| Calculated Gallium           | 14.4174           |
| Measured Weighing Pan        | 0.8275 ± 0.0002   |
| Measured Pan plus In         | 5.5184 ± 0.0002   |
| Measured Actual Indium       | 4.6909 ± 0.0002   |
| Expected Beaker plus Ga      | 44.7163           |
| Measured Beaker plus Ga      | 44.71334 ± 0.0002 |
| Measured Actual Gallium      | 14.4145 ± 0.0003  |

## 4.2 – Water Susceptibility Measurements

Distilled water was used to perform reference measurements. The MSB reads the magnetic susceptibility of the tube plus air plus water. Subtracting the reading of the empty tube from the sample tube does not properly correct for the susceptibility of the air displaced by the sample. Therefore the empty dry tube was used to measure the magnetic susceptibility of the tube plus air. The average magnetic susceptibility of the tube without water was  $-0.440 \times 10^{-6}$  cgs volume.

Air is paramagnetic because it consists of 20.9% oxygen. Therefore, the magnetic susceptibility of air is temperature dependent and the correct susceptibility corresponding to the average temperature of the experiment during the measurement must be used. The magnetic susceptibility for air was calculated for each batch at each run at the average temperature of the specific run and sample, summarized in Table 8 based on reference [20], and shown in Equation (5).

$$\chi_{air}(T) = \chi(293.15) \cdot \left( \frac{293.15 \text{ K}}{273.15 \text{ K} + T [k]} \right)^2, \quad \chi(293.15) = 0.029 \times 10^{-6} \text{ (cgs volume)} \quad (5)$$

The air-corrected magnetic susceptibility values were then used to consider for temperature and tilt correction respectively. The average corrected water measurements are summarized and plotted in Figures 9-11. Based on Figure 9, the temperature inside the shielding fluctuates within  $\pm 0.005^\circ\text{K}$  which is within the desired limit although the outside temperature fluctuates within  $\pm 0.206^\circ\text{K}$  over the first minute. The average magnetic susceptibility of the distilled water is  $(-0.669 \pm 0.004) \times 10^{-6}$  cgs volume which is within 7% of the literature value  $-0.712 \times 10^{-6}$  [19]. The 7% corresponds to

error margin which is due to limits in the sensitivity of the balance itself. It should be also considered that the measurements are within the order of  $0.001 \times 10^{-6}$  (cgs). Figure 10-11 show there was no visible tilt of the MSB within the limits of precision during the reference measurement.

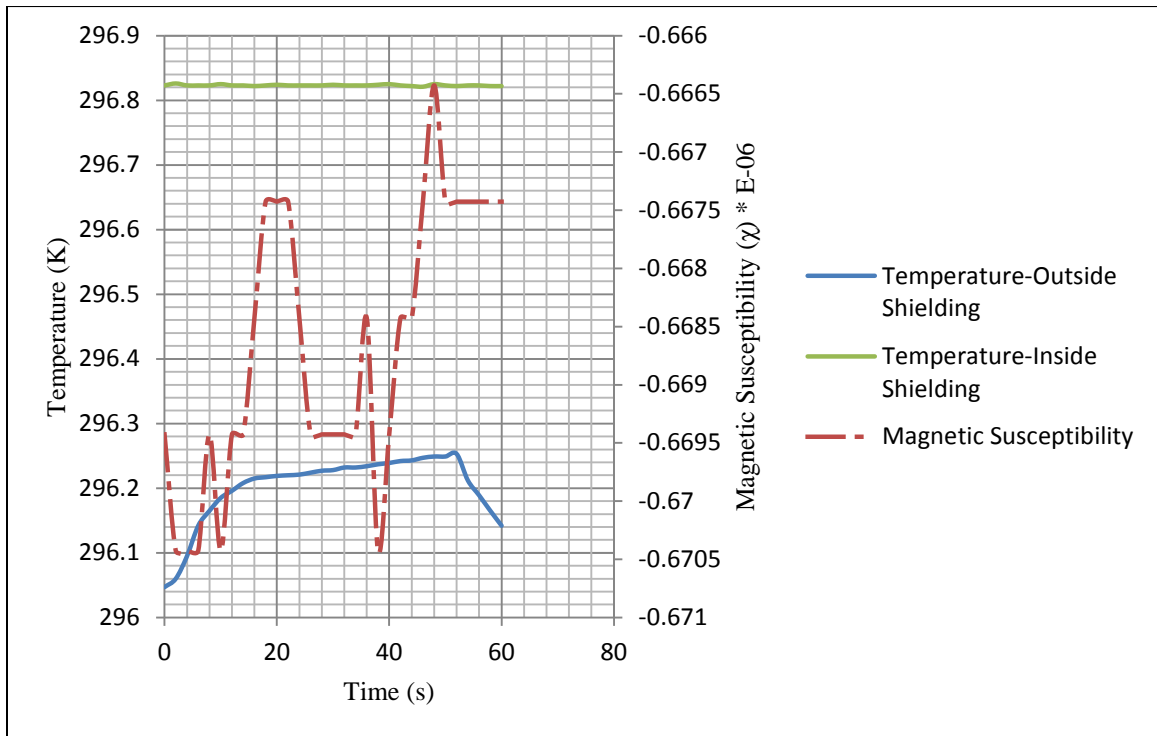


Figure 9- Fluctuations of  $\chi$  and T over 60 seconds for water measurements

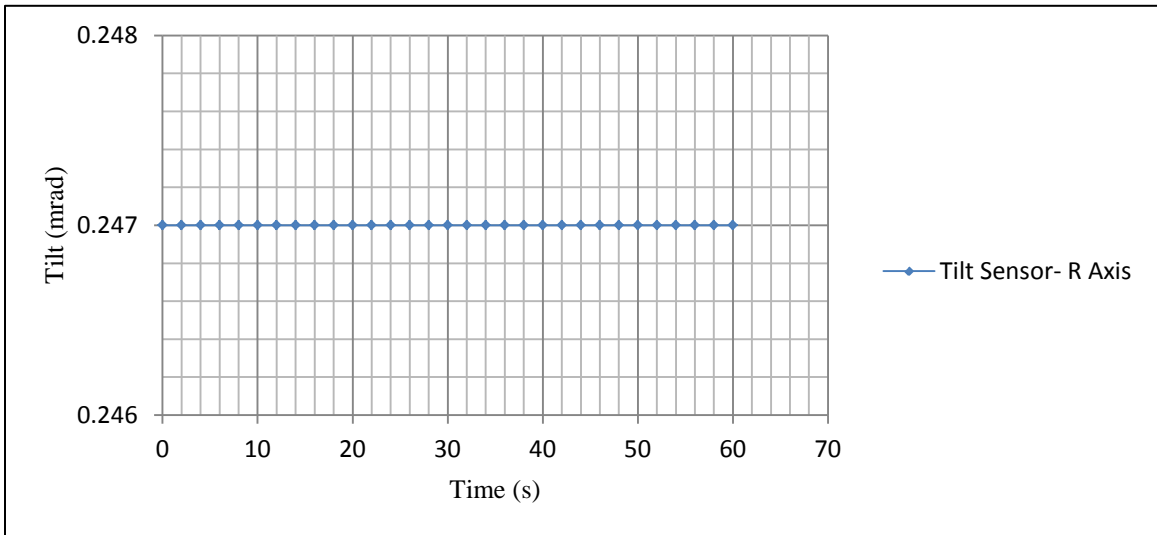


Figure 10- Tilt measurement of Roll axis for water over 60 seconds

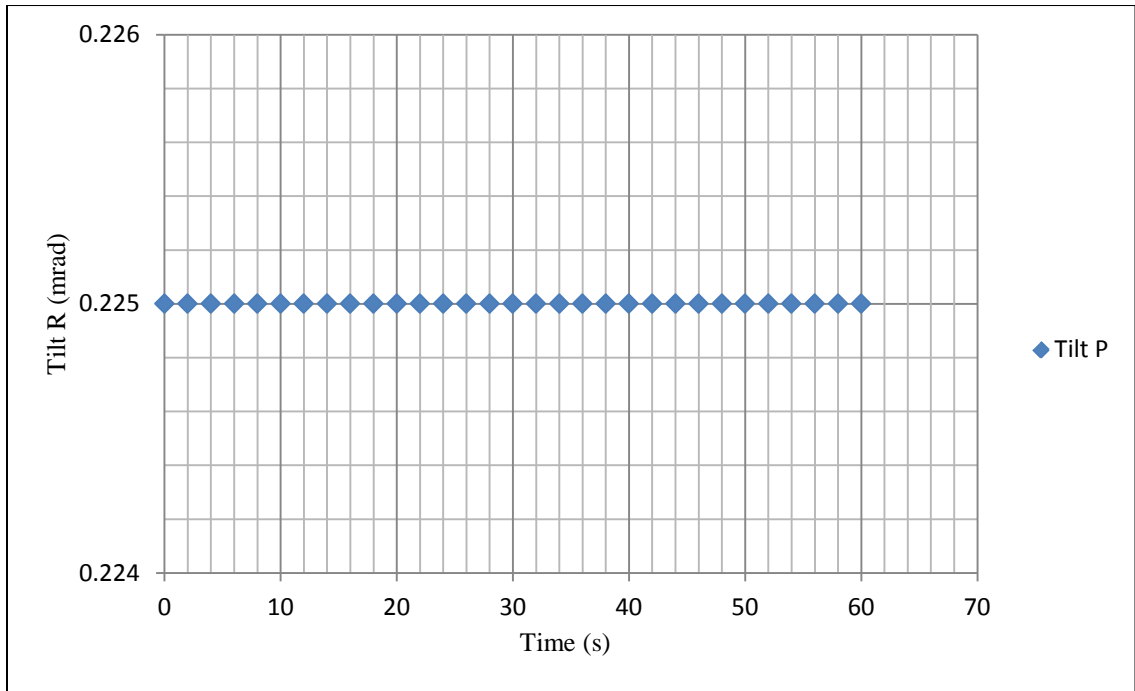


Figure 11- Tilt measurement of Pitch axis for water over 60 seconds



### 4.3 – Ga-In Alloys Measurements

The measured Ga-In alloy sample NMR tubes contained 5, 10, 12, 13.4, and 16.5 In atomic percent by calculation. The readings of the empty tubes were subtracted from the alloy samples and were corrected for the susceptibility of the air displaced by the sample. The average magnetic susceptibility of the tube without the water was  $-0.4233 \times 10^{-6}$  cgs volume. As correction for susceptibility of the air is temperature dependent, the correction for the average temperatures of each sample is summarized in Table 8 for all the measurements.

Table 8- Average temperatures (°K) used for air correction

| Alloys              | Measurement_1   | Measurement_2   | Measurement_3   | Measurement_4   |
|---------------------|-----------------|-----------------|-----------------|-----------------|
| Ga-In, 5 %<br>In    | 295.823 ± 0.005 | 295.867 ± 0.007 | 296.962 ± 0.004 | 297.226 ± 0.004 |
| Ga-In, 10 %<br>In   | 295.861 ± 0.006 | 295.894 ± 0.005 | 296.954 ± 0.005 | 297.238 ± 0.006 |
| Ga-In, 12%<br>In    | 295.895 ± 0.006 | 295.853 ± 0.004 | 296.946 ± 0.005 | 297.251 ± 0.005 |
| Ga-<br>In,13.4%In   | 295.926 ± 0.004 | 295.836 ± 0.006 | 296.937 ± 0.004 | 297.265 ± 0.006 |
| Ga-In, 16.5<br>% In | -               | 296.191 ± 0.005 | 296.926 ± 0.005 | 297.277 ± 0.004 |

The air-corrected magnetic susceptibility values were then considered for temperature correction and tilt correction respectively. The corrected magnetic susceptibility values were then averaged for each sample's run and the total average of the averaged corrected magnetic susceptibility values are reported in Table 9. Correcting for temperature an average temperature of 296.926 which is the average temperature of

all runs for the sample with 16.5 In percent was chosen for reference temperature correction in Equation (6).

$$\chi_m(T_1) = \chi_m(T_m) + \alpha \left( \frac{\delta \chi_{Ga}}{\delta T} \right) (T_m - T_1) + \beta \left( \frac{\delta \chi_{In}}{\delta T} \right) (T_m - T_1) \quad (6)$$

where  $T_1$  is the reference temperature,  $T_m$  is the average temperature of each run for each sample,  $\alpha$  is volume percent Ga in each batch,  $\frac{\delta \chi_{Ga}}{\delta T} = 0.24354 \times 10^{-8} \left( \frac{cgs}{K} \right)$  is Gallium temperature dependency constant [11],  $\beta$  is volume percent In in each batch, and  $\frac{\delta \chi_{In}}{\delta T} = 0.125 \times 10^{-8} \left( \frac{cgs}{K} \right)$  is Indium temperature dependency constant [21]. Equation 7 illustrates the linear relationship between  $\Delta \chi$  and Temperature variation.

$$\Delta \chi = A \Delta T \quad (7)$$

where  $\Delta \chi = \chi_m(T_1) - \chi_m(T_m)$ ,  $A = \left[ \alpha \left( \frac{\delta \chi_{Ga}}{\delta T} \right) + \beta \left( \frac{\delta \chi_{In}}{\delta T} \right) \right]$  which is a constant, and  $\Delta T = (T_m - T_1)$ .

Magnetic susceptibility correction for tilt R and tilt P, the reference values  $\theta_1 = 0.247$  (mrad) for tilt in Roll axis and  $\varphi_1 = 0.222$  (mrad) for tilt in Pitch axis were used respectively Equation (8).

$$\chi_m(\theta_1, \varphi_1) = \chi_m(\theta_m, \varphi_m) + \frac{\delta \chi}{\delta \theta} (\theta_m - \theta_1) + \frac{\delta \chi}{\delta \varphi} (\varphi_m - \varphi_1) \quad (8)$$

where  $\theta_1, \varphi_1$  are reference values for tilt R and P respectively,  $\frac{\delta \chi}{\delta \theta} = 5 \times 10^{-6} \left( \frac{cgs}{mrad} \right)$  tilt R dependency of magnetic susceptibility which is equal to  $\frac{\delta \chi}{\delta \theta}$ , tilt P dependency of

magnetic susceptibility. Although tilt variation would affect the magnetic susceptibility measurements, our tilt variation was sufficiently small that did not affect the resulting magnet susceptibility value. Equation (9) illustrates the linear relationship between  $\Delta\chi$  and  $(\Delta\theta + \Delta\varphi)$ .

$$\Delta\chi = B (\Delta\theta + \Delta\varphi) \quad (9)$$

where  $\Delta\chi = \chi_m(T_1) - \chi_m(T_m)$ ,  $B = \frac{\delta\chi}{\delta\theta} = \frac{\delta\chi}{\delta\varphi}$ ,  $\Delta\theta = \theta_m - \theta_1$ , and  $\Delta\varphi = \varphi_m - \varphi_1$ .

The results for the magnetic susceptibility readings ( $\chi$ ), temperature fluctuations, and tilt fluctuations in Pitch and Roll axis are shown during 60 seconds for each batch in Figures 12-31 respectively. Originally, the measurements were taken for 5 minutes to check consistency of the device, although based on MSB manual the measurements should take less than 10 seconds. The reported data in this work is the first 60 seconds of the 5 minutes measurement for each sample. The average magnetic susceptibility for Ga-In alloys with various In atomic % is summarized in Table 9. This table reveals the maximum fluctuation of  $\chi_v$  among the trials for all batches which is  $\pm 0.045 \times 10^{-6}$  (cgs). This error is the maximum systematic drift which is calculated by subtracting the maximum  $\chi_v$  of all the runs from the minimum  $\chi_v$  of all runs. Figures 12, 13, 14, 15, and 16 illustrate the fluctuations in magnetic susceptibility measurements for each alloy during 60 seconds for all the runs. The variation during each specific run is much smaller than run to run variations.

Table 9- Averaged magnetic susceptibility measurements for Ga-In alloys (cgs volume)

| Alloys           | $(\chi_{\text{avg}} \pm \Delta\chi) \times 10^{-6}$ |
|------------------|---|
| Ga-In, 5 % In    | $-0.0602 \pm 0.0450$                                |
| Ga-In, 10 % In   | $-0.0953 \pm 0.0250$                                |
| Ga-In, 12 % In   | $-0.1062 \pm 0.0180$                                |
| Ga-In, 13.4 % In | $-0.1165 \pm 0.0140$                                |
| Ga-In, 16.5 % In | $-0.1256 \pm 0.0170$                                |

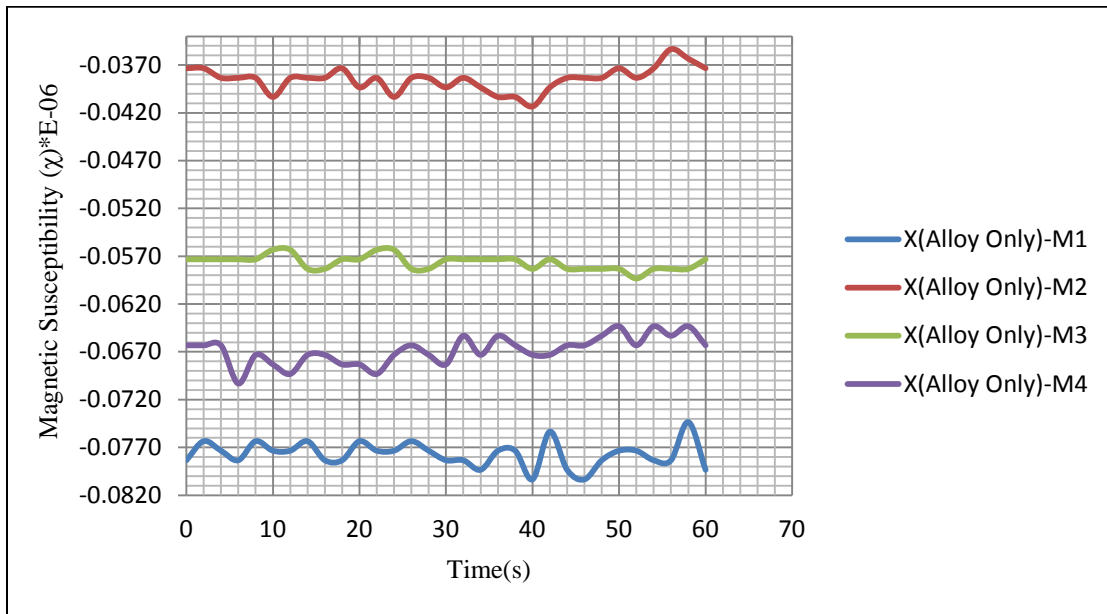


Figure 12- Magnetic susceptibility measurements for Ga-In 5% In over 60 (s)

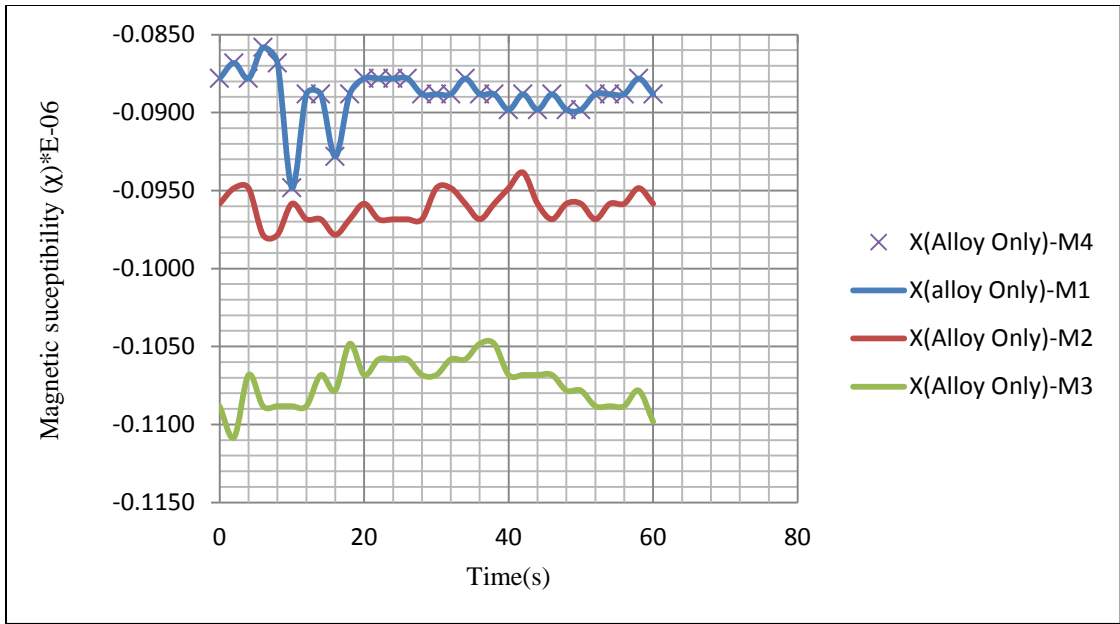


Figure 13- Magnetic susceptibility measurements for Ga-In 10% In over 60 (s)

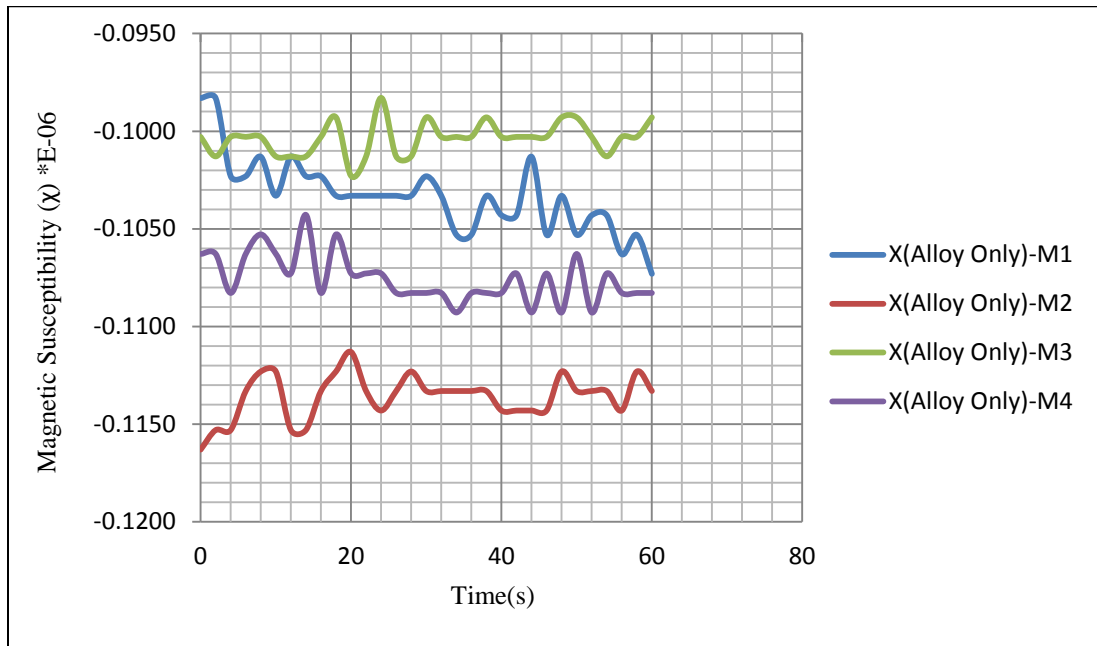


Figure 14- Magnetic susceptibility measurements for Ga-In 12% In over 60 (s)

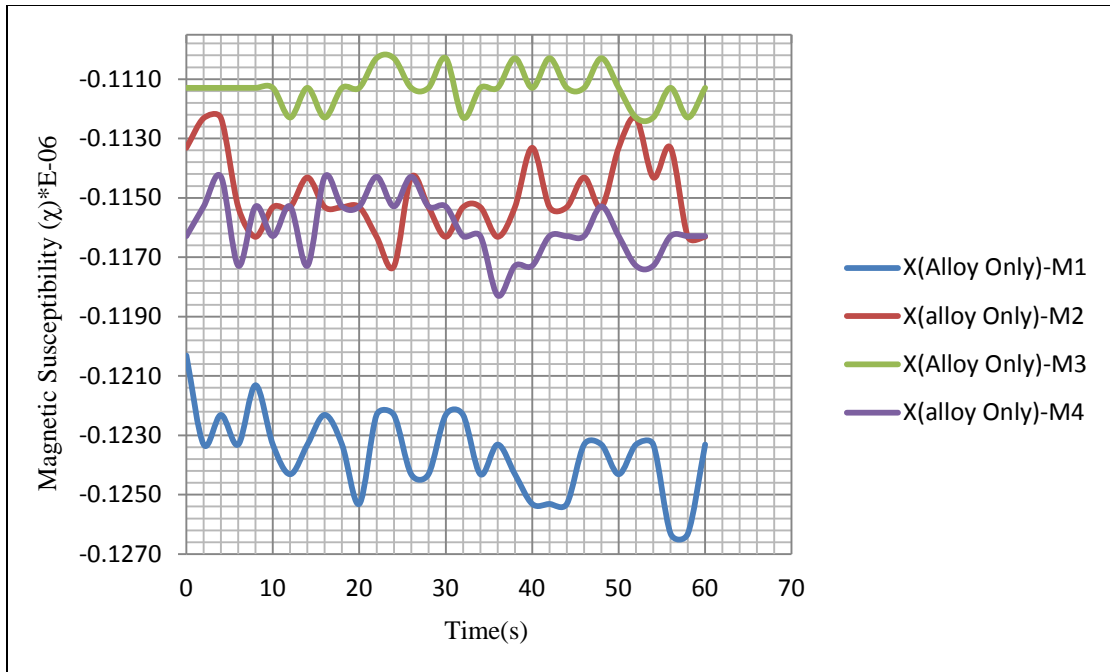


Figure 15- Magnetic susceptibility measurements for Ga-In 13.4% In over 60 (s)

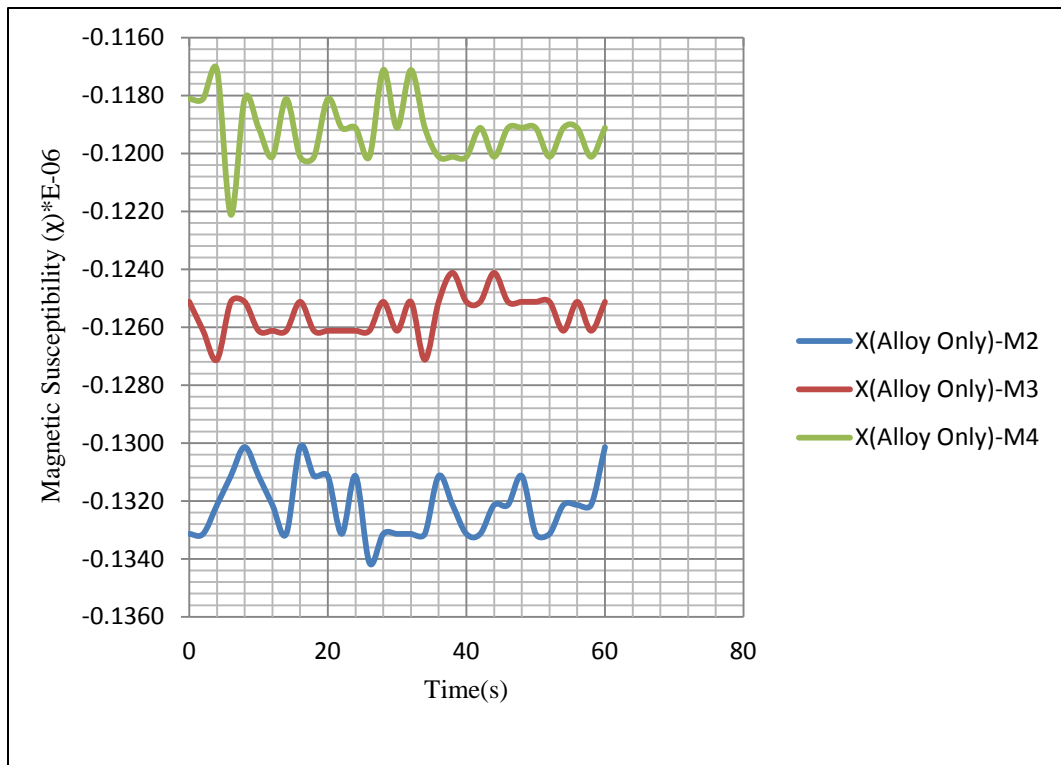


Figure 16- Magnetic susceptibility measurements for Ga-In 16.5% In over 60 (s)

The temperature variation in each measurement is summarized in Table 8 and shown in Figures 17, 18, 19, 20, and 21 with maximum error value of  $\pm 0.007$  °K.

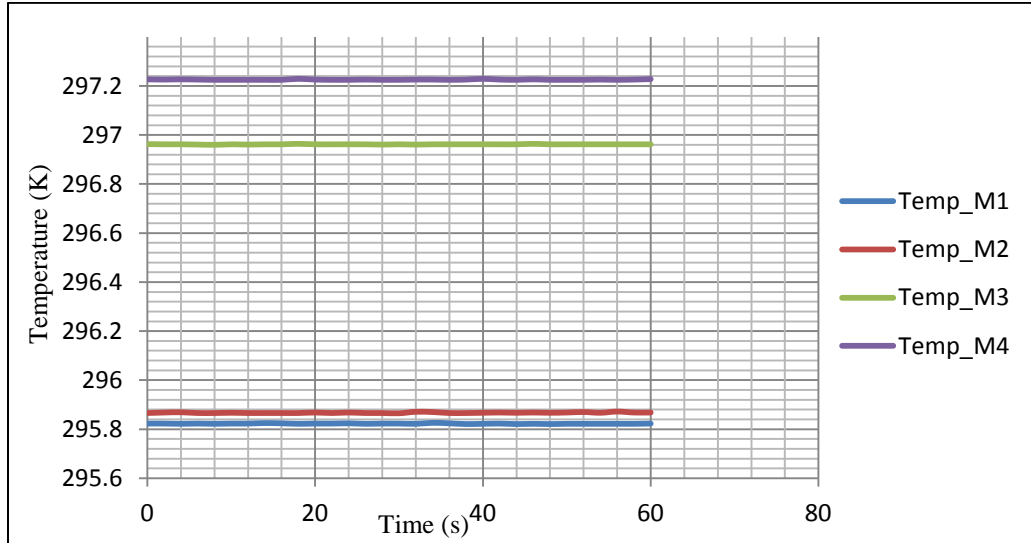


Figure 17- Temperature measurements for Ga-In, 5% In alloy over 60 (s)

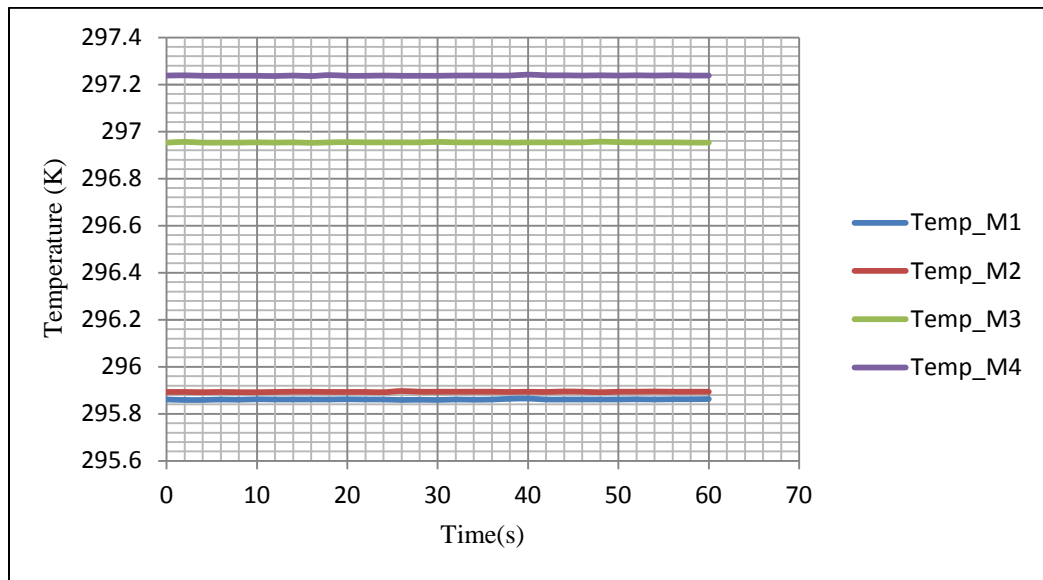


Figure 18- Temperature measurements for Ga-In, 10% In alloy over 60 (s)

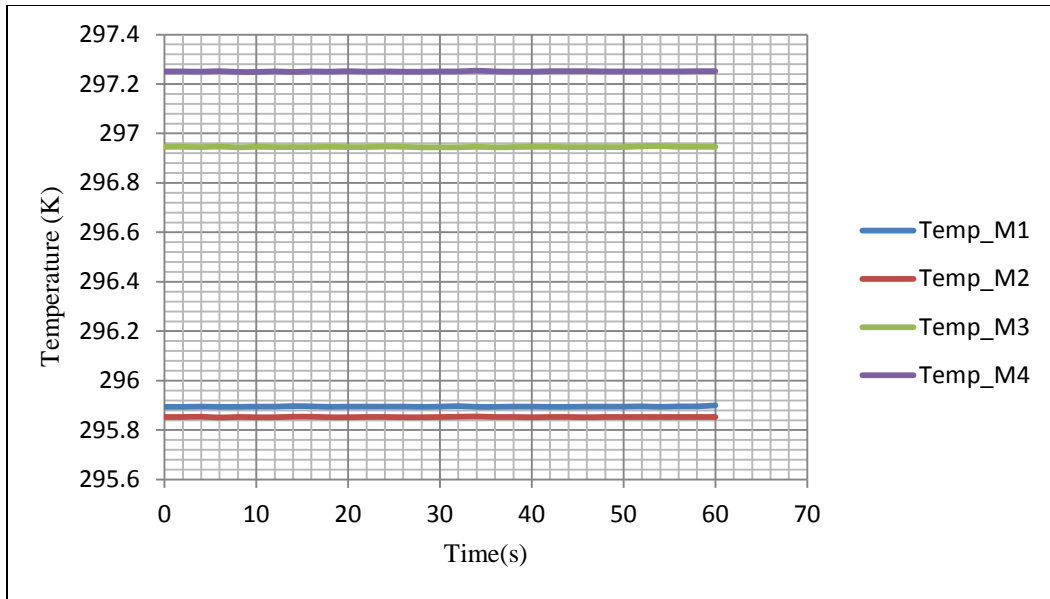


Figure 19- Temperature measurements for Ga-In, 12% In alloy over 60 (s)

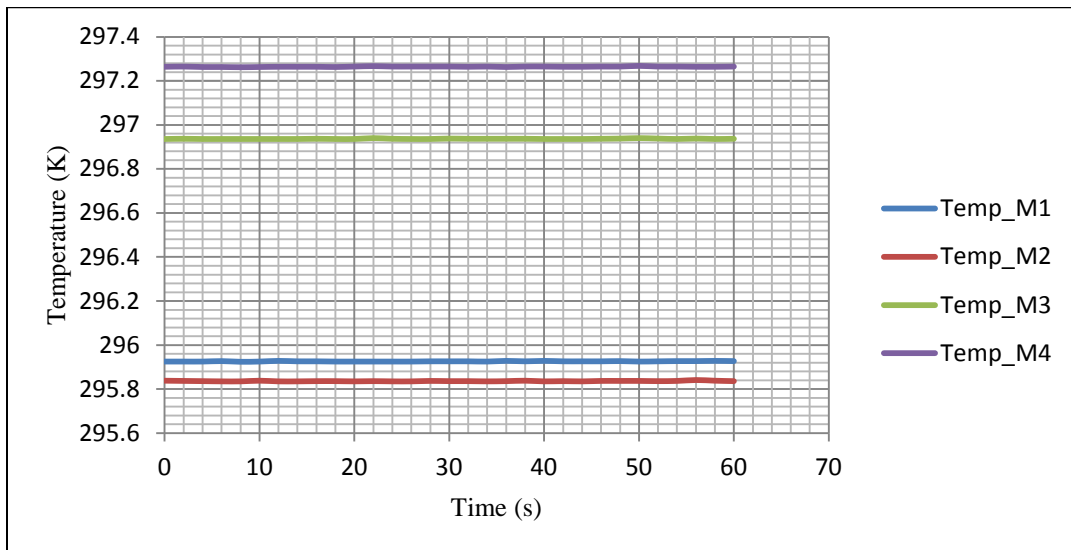


Figure 20- Temperature measurements for Ga-In, 13.4% In alloy over 60 (s)



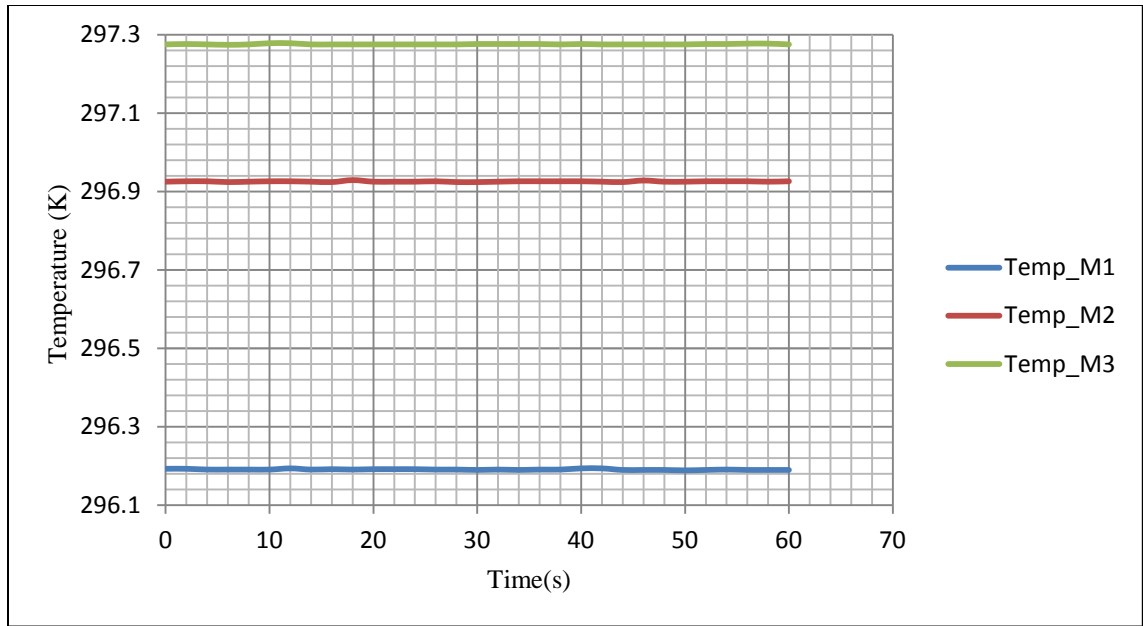


Figure 21- Temperature measurements for Ga-In, 16.5% In alloy over 60 (s)

The two-axis tilt sensor measurements Tilt-R and Tilt-P, shown in Figures 22-31, changed slightly among trials while there was no fluctuation in each measurement during the individual runs. The averaged measurements for Roll and Pitch axis tilts are summarized in Table 10 and Table 11 respectively. The MSB was initially calibrated for tilt with bidirectional device level. The values in Table 10 and Table 11 are initially of a leveled system and the variations was looked for from the reference state of  $\theta_1 = 0.247$  (mrad) for tilt in Roll axis (tilt R) and  $\phi_1 = 0.222$  (mrad) for tilt in Pitch axis (tilt P).

Table 10- Tilt measurements of Roll axis for Ga-In alloys (mrad)

| Alloys         | Tilt R_M1 | Tilt R_M2 | Tilt R_M3 | Tilt R_M4 |
|----------------|-----------|-----------|-----------|-----------|
| Ga-In 5% In    | 0.247     | 0.247     | 0.244     | 0.247     |
| Ga-In 10% In   | 0.247     | 0.247     | 0.244     | 0.247     |
| Ga-In 12% In   | 0.247     | 0.247     | 0.244     | 0.247     |
| Ga-In 13.4% In | 0.247     | 0.247     | 0.244     | 0.247     |
| Ga-In 16.5% In | -         | 0.246     | 0.244     | 0.247     |

Table 11- Tilt measurements of Pitch axis for Ga-In alloys (mrad)

| Alloys         | Tilt P_M1 | Tilt P_M2 | Tilt P_M3 | Tilt P_M4 |
|----------------|-----------|-----------|-----------|-----------|
| Ga-In 5% In    | 0.225     | 0.225     | 0.222     | 0.219     |
| Ga-In 10% In   | 0.225     | 0.225     | 0.221     | 0.219     |
| Ga-In 12% In   | 0.226     | 0.225     | 0.222     | 0.219     |
| Ga-In 13.4% In | 0.226     | 0.225     | 0.222     | 0.219     |
| Ga-In 16.5% In | -         | 0.223     | 0.222     | 0.220     |

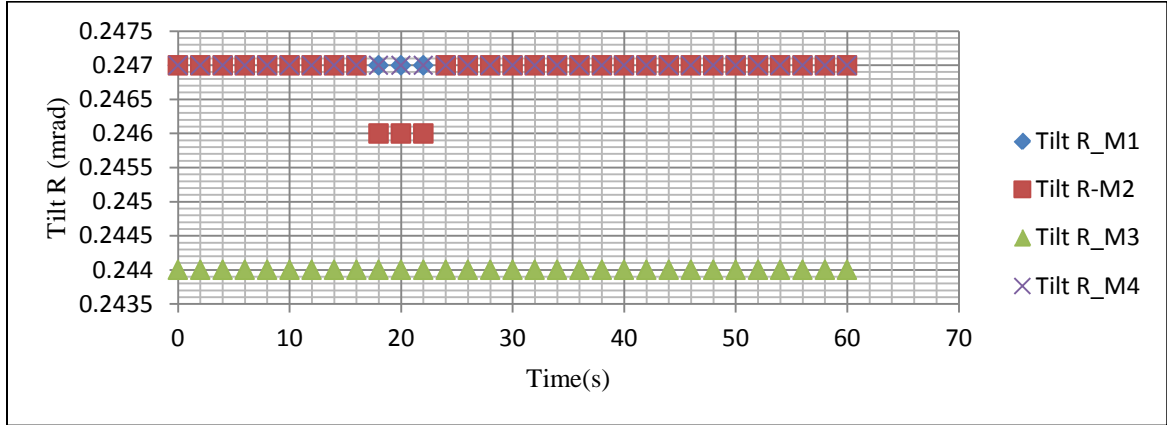


Figure 22- Tilt measurements of Roll axis for Ga-In 5% In over 60 (s)

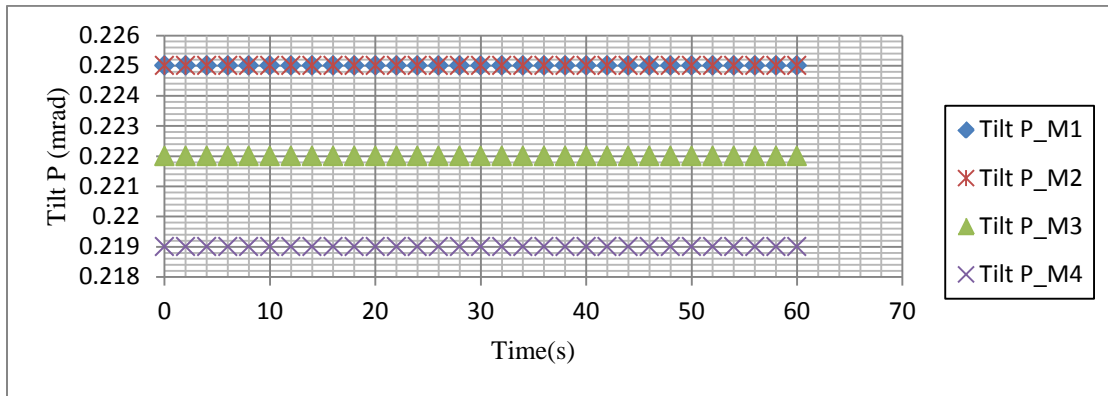


Figure 23- Tilt measurements of Pitch axis for Ga-In 5% In over 60 (s)

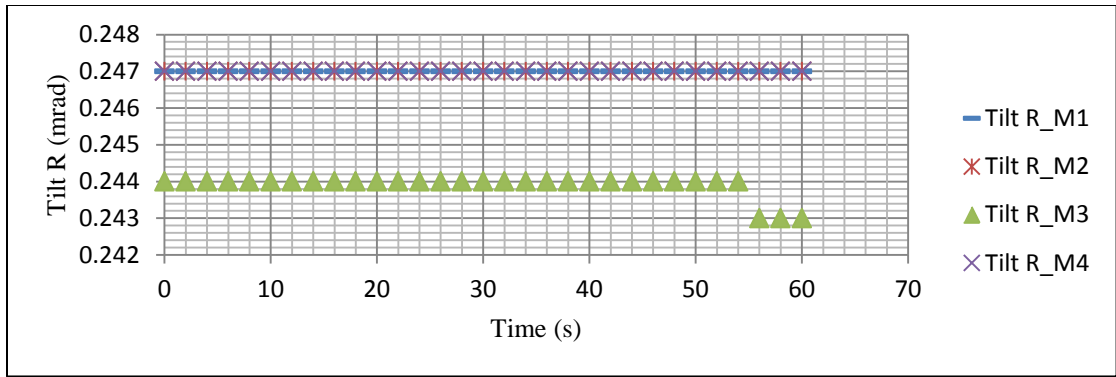


Figure 24- Tilt measurements of Roll axis for Ga-In 10% In over 60 (s)

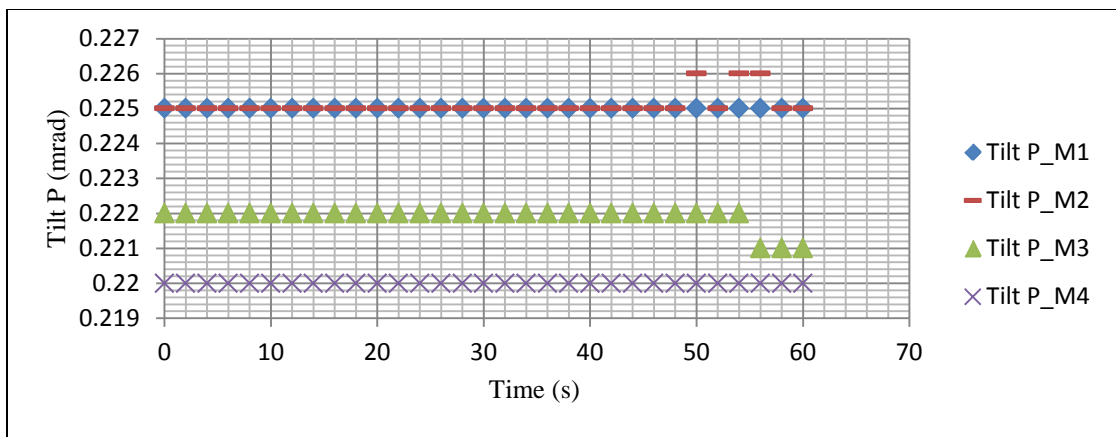


Figure 25- Tilt measurements of Pitch axis for Ga-In 10% In over 60 (s)

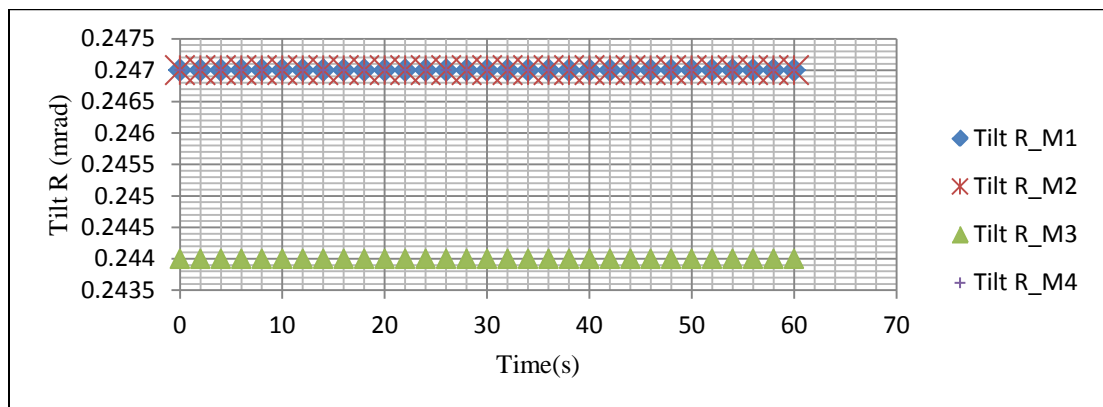


Figure 26- Tilt measurements of Roll axis for Ga-In 12% In over 60 (s)

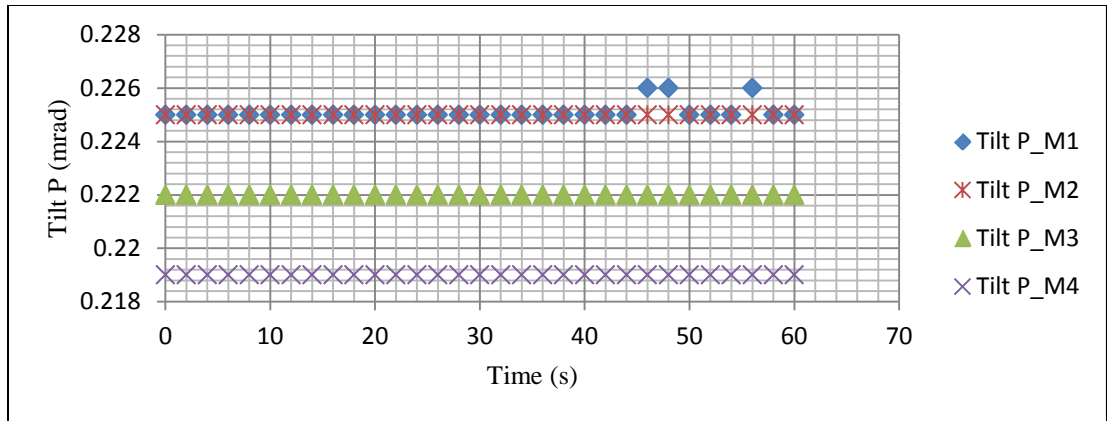


Figure 27- Tilt measurements of Pitch axis for Ga-In 12% In over 60 (s)

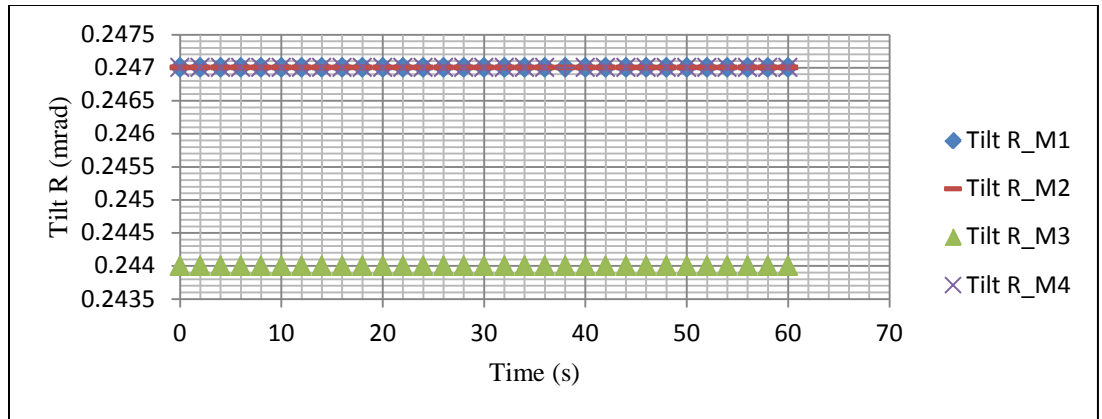


Figure 28- Tilt measurements of Roll axis for Ga-In 13.4% In over 60 (s)

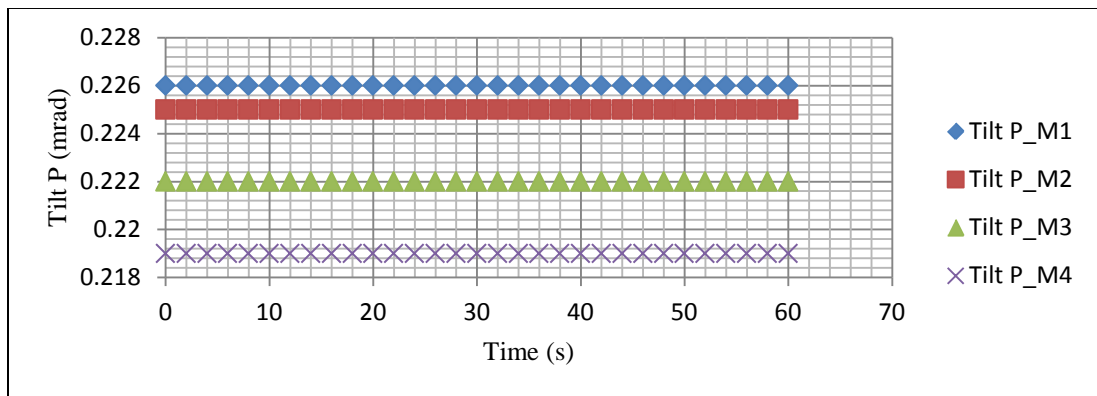


Figure 29- Tilt measurements of Pitch axis for Ga-In 13.4% In over 60 (s)

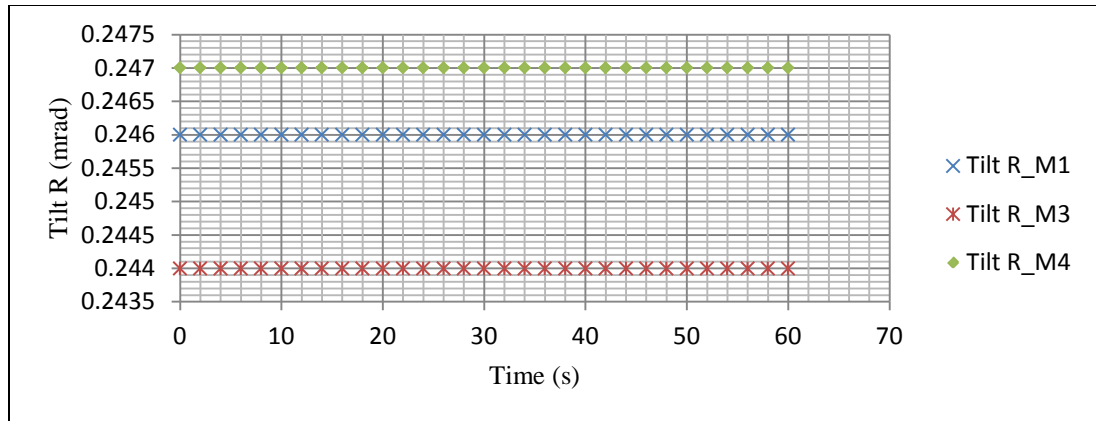


Figure 30- Tilt measurements of Roll axis for Ga-In 16.5% In over 60 (s)

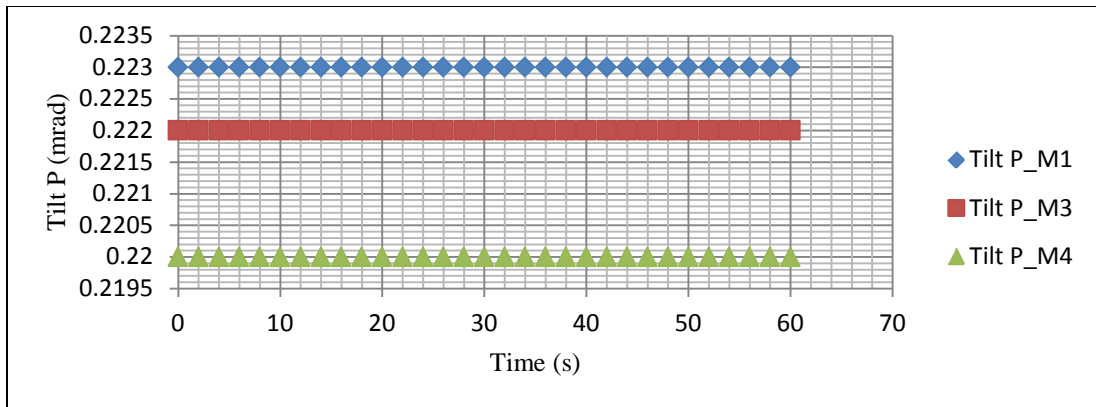


Figure 31- Tilt measurements of Pitch axis for Ga-In 16.5% In over 60 (s)

Figure 32 illustrates the average magnetic susceptibility for all the Ga-In alloy batches with 5, 10, 12, 13.4, and 16.5 atomic percent Indium that is summarized in Table 9.

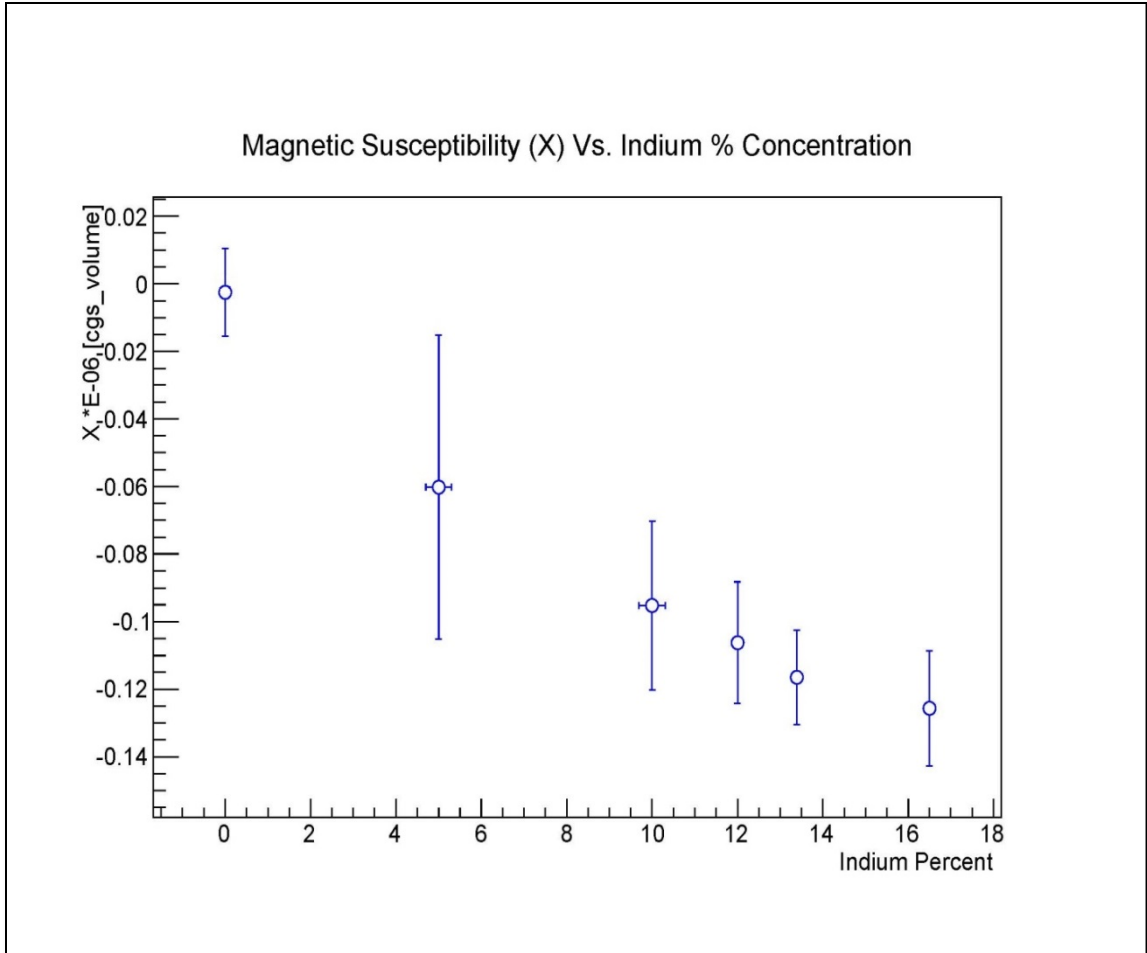


Figure 32- Average magnetic susceptibility Vs. Indium Concentration

To test for non-Linear behavior of the value of  $\chi$  with percent Indium, a polynomial form of  $y = P_2x_2 + P_1x + p_0$  was fitted. This fit is shown as a solid line in Figure 33. The fit parameters are  $P_2 = 0.00029 \pm 0.00031$ ,  $P_1 = -0.01227 \pm 0.00467$ , and  $p_0 = -0.00261 \pm 0.01292$ . The  $P_2$  parameter is consistent with zero within uncertainties and therefore demonstrates that our data does not exhibit significant non-linearity.

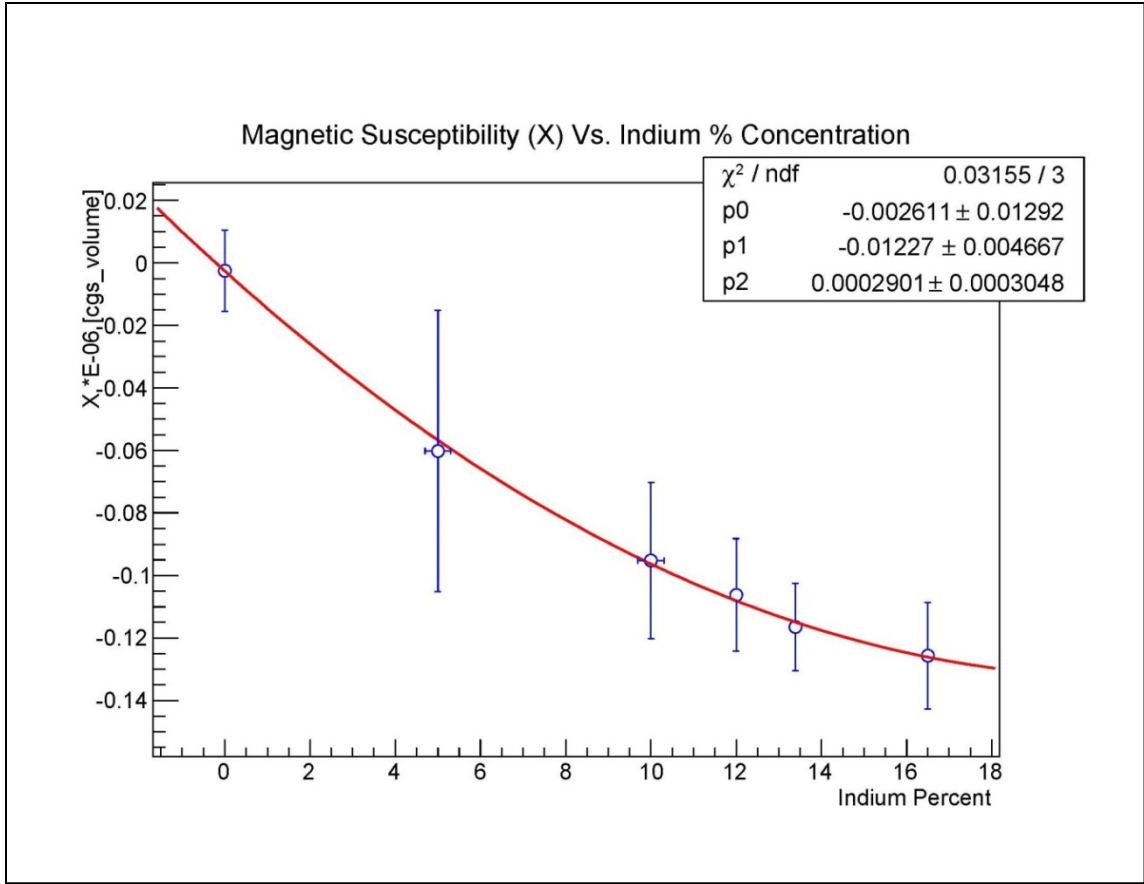


Figure 33- Magnetic susceptibility Vs. In Concentration with Polynomial fit

Therefore the  $\chi$  Vs. Indium concentration plot was refitted with a linear function of the form  $y = C_1x + C_0$  and we found  $C_1 = -0.00796 \pm 0.00111 \left(\frac{cgs}{cm^3}\right)$ ,  $C_0 = -0.00580 \pm 0.01248 (cgs)$  as shown by the solid line in Figure 34. It is notable that the y-intercept is consistent with zero within uncertainties.

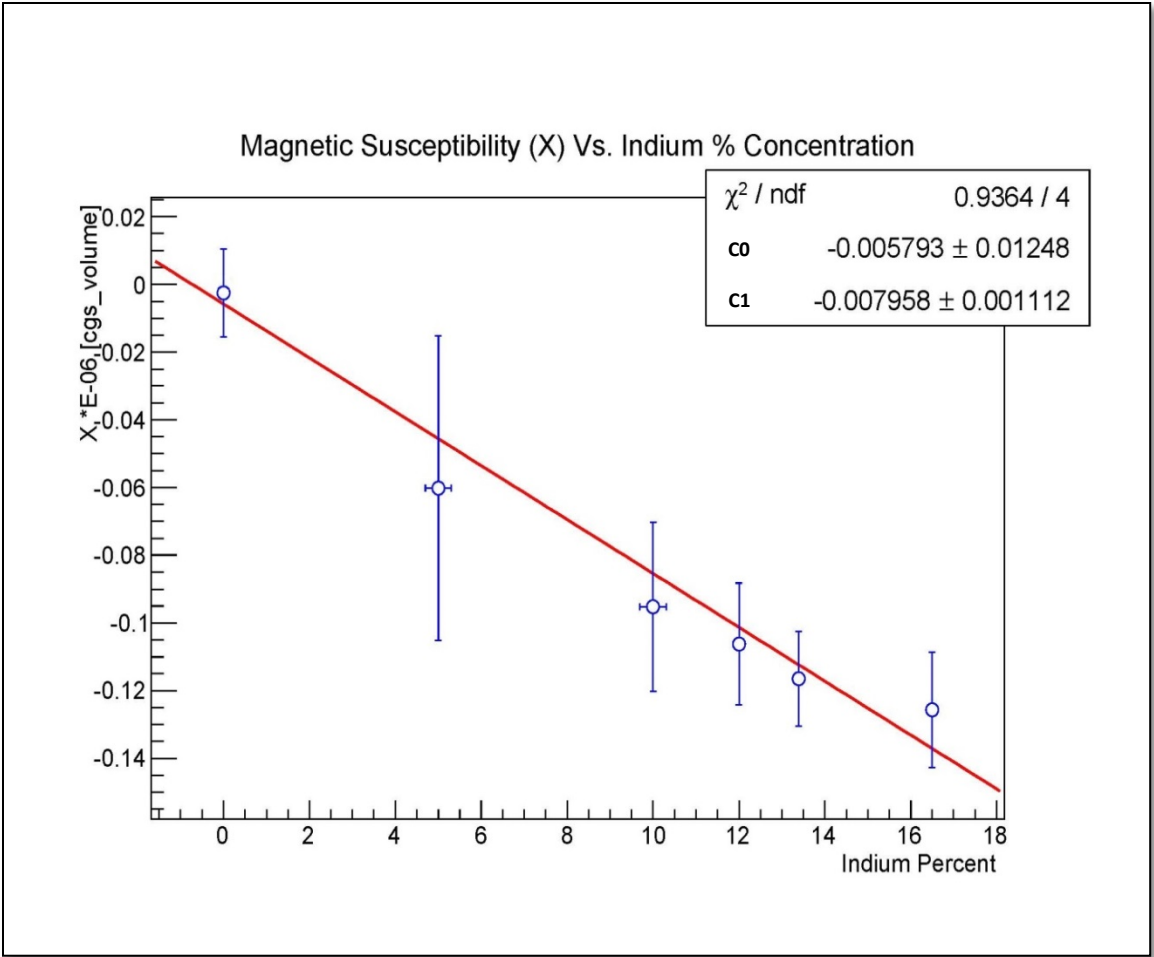


Figure 34- Magnetic susceptibility Vs. In Concentration with Linear fit



#### 4.4 – Discussion

This research project has proven the hypothesis of significant low magnetic susceptibility of Ga-In Alloys by studying various batches with different In percentage. In fact, Ga-In alloys have magnetic susceptibility that is 5 to 10 times smaller than the magnetic susceptibility ( $\chi_v$ ) of water  $-0.72 \times 10^{-6}$  cgs) and at the same time, has a larger number of fermions, neutrons and protons, per unit volume than water. It is therefore a much better material to use in future fifth-force measurements where fermion interactions are being studied.

The water magnetic susceptibility measurement shows that the susceptibility balance absolute accuracy is within the 7% of the literature value of pure water. This error margin is due to limits of the sensitivity of the balance itself. We were able to achieve thermal (0.005 °K) and tilt (0.001 mrad) stability desired for the reproducible operation of the susceptibility measurement. Ideally, there should not be any fluctuation is temperature and tilt as the MSB is a mechanical torsion balance. While no variation is impossible, significantly small fluctuations were reached that have negligible effect on the considerably precise scale measurements. The magnetic susceptibility of the measured Ga-In alloy of 16.5 % In is  $(-0.13 \pm 0.017) \times 10^{-6}$  (cgs) volume susceptibility which is within the uncertainties of literature value  $0.15 \times 10^{-6}$  based on reference [19] (in this reference the error margin is not reported). We also examined the dependence of our measured  $\chi$  with the atomic % of Indium and found a linear dependence following the model  $y = C_1x + C_0$  in Figure 34 with coefficients  $C_1 = -0.00796 \pm 0.00111$  ( $\frac{cgs}{cm^3}$ ),

$C_0 = -0.00580 \pm 0.01248$  (*cgs*). In this thesis we have developed Ga- In alloys with much lower diamagnetism in comparison to water.

Our future work will involve using Ga- In alloys to study the NMR frequency shift as the mass is moved near and far from the polarized ensemble to study the improvements on the coupling constant which sets a direct limit on the important “axion window”.

## LIST OF REFERENCES

1. P. H. Chu, A.D., C. B. Fu, H. Gao, R. Khatiwada, G. Laskaris, K. Li, E. Smith, W. M. Snow, H. Yan, and W. Zheng, "*Laboratory search for spin-dependent short-range force from axionlike particles using optically polarized  $^3\text{He}$  gas*". Physical Review D, 2013. **87**(011105): p. 1-4.
2. Ravaine, B., "*Violation of parity and time-reversal in atoms and molecules*", in *Department of Physics*. (2007), University of Nevada, Reno. p. 1-3.
3. W. Zheng, H.G., B. Lalremruata, Y. Zhang, G. Laskaris, W. M. Snow, and C. B. Fu, "*Search for spin-dependent short-range force between nucleons using optically polarized  $^3\text{He}$  gas*". Physical Review D, 2012. **85**(031505).
4. J. E. Moody, F.W., "*New macroscopic forces?*". Physical Review D, 1984. **30**(130).
5. A. N. Youdin, D.K., Jr., K. Jagannathan, and L. R. Hunter, "*Limits on Spin-Mass Couplings within the Axion Window*". Physical Review Letters, 1996. **77**(2170).
6. R. C. Ritter, L.I.W., and G. T. Gillies, "*Search for anomalous spin-dependent forces with a polarized-mass torsion pendulum*". Physical Review Letters, 1993. **70**(701).
7. S. Baeßler, V.V.N., K. V. Protasov, and A. Yu. Voronin, "*Constraint on the coupling of axionlike particles to matter via an ultracold neutron gravitational experiment*". Physical Review D, 2007. **75**(075006).
8. A. K. Petukhov, G.P., and R. Golub, "*Comment on ‘Limits on possible new nucleon monopole-dipole interactions from the spin relaxation rate of polarized  $^3\text{He}$  gas’*". Physical Review D, 2011. **84**(058501).
9. M. Bulatowicz, R.G., M. Larsen, J. Mirijanian, C. B. Fu, E. Smith, W. M. Snow, H. Yan, and T. G. Walker, "*Laboratory Search for a Long-Range T-Odd, P-Odd Interaction from Axionlike Particles Using Dual-Species Nuclear Magnetic Resonance with Polarized  $^{129}\text{Xe}$  and  $^{131}\text{Xe}$  Gas*". Physical Review Letters, 2013. **111**(102001).
10. K. Tullney, F.A., M. Burghoff, W. Heil, S. Karpuk, W. Kilian, S. Knappe-Grüneberg, W. Müller, U. Schmidt, A. Schnabel, F. Seifert, Yu. Sobolev, and L. Trahms, "*Constraints on Spin-Dependent Short-Range Interaction between Nucleons*". Physical Review Letters, 2013. **111**(100801).
11. K. SUZUKI, O.U., "*Knight Shift, Magnetic Susceptibility and Electrical Resistivity of Pure Gallium and Gallium-Indium Eutectic Alloy in the Normal and Supercooled Liquid State*". Physical Chemistry Solids, 1971. **32**: p. 1801-1810.
12. Matthey, J., "*MSB-Auto/ Magnetic Susceptibility Balance*". (2006): USA.

13. J.T. Bushberg, J.A.S., E. M. Leidholdt, & J. M. Boone, "*The Essential Physics of Medical Imaging*". Third Edition ed. (2012), Philadelphia: Lippincott Williams & Wilkins.
14. J A. Pople, W.G.S., & H. J. Bernstein, "*High- resolution Nuclear Magnetic Resonance*". (1959), USA: McGraw-Hill Book Company, Inc.
15. Mulay, L.N., "*Magnetic Susceptibility*". (1963), USA: John Wiley & Sons, Inc.
16. B. P. Pashaey, V.V.S., "*Magnetic susceptibility of gallium-indium alloys in liquid state*". Soviet Physics Journal, 1973. **16**(4): p. 565-566.
17. M.F. Dumke , T.A.T., R.A. Weller, R.M. Hously, E.H. Cirlin, "Sputtering of the Gallium-Indium Alloy in Liquid Phase". Surface Science, 1983. 124: p. 407-422.
18. J. Kim, H.S., J. Cho,& S. Park, "Effect of Oxidation on Indium Solderability". Journal of Electronic Materials, (2008). 37(4).
19. Z. Skokanová, J.K., M. Rákoš "Effect of water of crystallization on magnetic properties of MgSO<sub>4</sub>". Czechoslovak Journal of Physics, 1978. 28(2): p. 220-227.
20. Hey, S., "Magnetic resonance imaging as an instrument for temperature measurements during cancer treatment", in Mathematics and Natural Sciences. (2007), Universitat Greifswald: Greifswald, Germany.
21. B. N. Aleksandrov, B.I.V., and I. V. Svechkarev, "Temperature dependency of the magnetic susceptibility of Indium, Lead, and Tin Crystals". SOVIET PHYSICS JETP, 1960. 12(1).

Curriculum Vitae

**MARJAN KHOSRAVI**  
Email: Khosravm@umail.iu.edu

---

**EDUCATION**

- 2012- 2014      **Master of Science, Medical Physics**, (GPA=3.846)  
Indiana University, Bloomington, IN
- 2007- 2012      **Bachelor of Science, Solid State Physics**, (GPA=3.5)  
Shahid Beheshti University, Tehran, Iran

**REASEARCH  
EXPERIENCE**

- Aug.2014- Present      **Medical Physics Research consultant**  
ProNova Solutions - IU Health Proton Therapy Center
- Quality Assurance (QA) detector development testing to verify applicability and accuracy of the equipment and Pencil Beam Scanning (PBS) at Indiana University Health Proton Therapy Center
  - Participate in medical device certification testing based on FDA 510 K guidelines
  - Develop test protocols for formal medical equipment via verification and validation
  - Use X-ray Beam Metrology System (XRV-2020 Scintillator detector) for PBS testing through its manufactured scripting language
  - Collect and analyze the data with the resultant test reports with minimum supervision
- Aug.2013- Nov.2014      **Research Assistant**  
Indiana University Bloomington  
Development of Gallium-Indium Alloys, Nonmagnetic Test Masses for Spin-Dependent Short-Range Force Searches at Center for Exploration of Energy and Matter  
Indiana University Bloomington
- Synthesize and characterize physical properties of Gallium-Indium alloys
  - Factorial design for torsion balance Nuclear Magnetic Resonance (NMR)
  - Data acquisition and analysis for magnetic susceptibility measurements
- Aug.2013- Feb.2014      **Research Assistant**  
Indiana University Bloomington  
Implementing Local Image Statistics construction by using Python

**TEACHING  
EXPERIENCE**

- Feb.2014- Aug.2014      **Associate Instructor**, Development of TLD Experiment, Modern Physics Lab  
Indiana University Bloomington
- Radiating TLDs and GAF Chromic Films with the purpose of learning to work with TLD reader software, CCD100 Microdosimeter, and understanding the glow curve and its relation with dose for undergrad physics students
- Sept.2013- Dec.2013      **Teaching Assistant**, Fundamentals of Radiation Science  
Indiana University Bloomington
- Sept.2010- Jan.2011      **Teaching Assistant**, Electronics I  
Shahid Beheshti University, Tehran, Iran, Sept.2010- Jan.2011

## RELEVANT EXPERIENCE

Nov.2012- Dec.2012 **Digital Electronics Project:**Light Level Sensing Circuit with Audio Output  
Indiana University Bloomington

May.2011- Mar.2012 **Bachelor Degree Project:**Synthesis of Core Shell Particles Consisting of Cobalt Ferrite and Silica as Model Ferrofluids [CoFe<sub>2</sub>O<sub>4</sub>-SiO<sub>2</sub> CoreShell Particles]  
Shahid Beheshti University,Tehran, Iran, May.2011- Mar.2012

## SKILLS

- Technical Softwares: Proficient in R, ROOT, Logger Pro, LaTeX, Maester, ImageJ, Mathematica, MathType, Adobe Illustrator, Photoshop, EndNote, Agile software development, Jazz transform software & systems delivery
- Imaging/ Treatment planning Softwares: XRV-20XX detector software, Manufacture scripting language-WinLVS software, ProfileView software, BeamWorks software, Varian Aria, Eclipse
- Programming: Python, LabVIEW

## MEMBERSHIP

2012- Present Member, American Association of Physicist in Medicine (AAPM)  
2012- Present Member, Association of Iranian Physicist in Medicine (AIPM)  
2014- Present Member, American Physical Society (APS)  
2012- Present Member, Center of Excellence for Women in Technology (CEWiT)  
2014- Present Member, Medical and Biological Physics Student Organization (MaBPSO) at Indiana University

## PUBLICATIONS

R. Khatiwada, **M.Khosravi**, W. M. Snow, Non-magnetic Masses, Manuscript in progress for publication, (2014)

## PRESENTATIONS

Mar.2014 **Marjan Khosravi**, Development of Gallium-Indium, Non Magnetic Test Masses for Spin-Dependent Short-Range Force Searches, Oral Presentation, American Physical Society (APS), (Pending)

Sept.2014 **M.Khosravi**, R. Khatiwada, W. M. Snow, Gallium-Indium, Non-magnetic Test Masses for Fifth force Searches, Poster Presentation, Indiana Clinical and Translational Science Institute (CTSI)

Apr.2014 **M.Khosravi**, R. Khatiwada, W. M. Snow, Gallium- Indium Alloys as Non-magnetic Test Masses for Fifth force Searches, Poster Presentation, The 2014 American Association of Physicist in Medicine Ohio River Valley Chapter (AAPM-ORVC) Spring Clinical Meeting, (Apr. 2014)

Sept.2011 M.Houshiar, **M.Khosravi**, The Effect of Metal Impurity on Crystal Structure of Inter Metallic Alloy, Poster Presentation, Annual Physics Conference of Iran-Orumieh, Sept. 2011

## AWARDS

- **Provost Women in Science Travel Award**, *The 2013 Annual meeting of American Association of Physicists in Medicine (AAPM), Indiana University Bloomington*
- **Provost Women in Science Travel Award**, *The 2014 AAPM ORVC Spring Clinical Meeting , Indiana University Bloomington 2014*